British Journal of Cancer (2005) 92, 1942–1947

www.bjcancer.com

Quantitative relationship between functionally active telomerase and major telomerase components (hTERT and hTR) in acute leukaemia cells

JH Ohyashiki*[,1], H Hisatomi[2], K Nagao[3], S Honda[4], T Takaku[4], Y Zhang[4], G Sashida[4] and K Ohyashiki[4]

[1]Intractable Immune System Diseases Research Center, Tokyo Medical University, 6-7-1, Nishishinjuku, Shinjuku, Tokyo 160-0023, Japan; [2]Analytical Center for Medical Science, SRL Inc., Tokyo, Japan; [3]Center for Molecular Biology and Cytogenetics, SRL Inc., Tokyo, Japan; [4]First Department of Internal Medicine, Tokyo Medical University, Tokyo, Japan

Functionally active telomerase is affected at various steps including transcriptional and post-transcriptional levels of major telomerase components (hTR and human telomerase reverse transcriptase (hTERT)). We therefore developed a rapid and sensitive method to quantify hTERT and its splicing variants as well as the hTR by a Taqman real-time reverse transcriptase–polymerase chain reaction to determine whether their altered expression may contribute to telomere attrition *in vivo* or not. Fresh leukaemia cells obtained from 38 consecutive patients were used in this study. The enzymatic level of telomerase activity measured by TRAP assay was generally associated with the copy numbers of full-length hTERT $+\alpha+\beta$ mRNA ($P=0.0024$), but did not correlate with hTR expression ($P=0.6753$). In spite of high copy numbers of full-length hTERT mRNA, telomerase activity was low in some cases correlating with low copy numbers of hTR, raising the possibility that alteration of the hTR:hTERT ratio may affect functionally active telomerase activity *in vivo*. The spliced nonactive hTERT mRNA tends to be lower in patients with high telomerase activity, suggesting that this epiphenomenon may play some role in telomerase regulation. An understanding of the complexities of telomerase gene regulation in biologically heterogeneous leukaemia cells may offer new therapeutic approaches to the treatment of acute leukaemia.
British Journal of Cancer (2005) **92,** 1942–1947. doi:10.1038/sj.bjc.6602546 www.bjcancer.com
Published online 12 April 2005

Keywords: telomerase; hTERT; splicing variants; hTR

Human telomerase reverse transcriptase (hTERT) is an essential component of the holoenzyme complex that adds telomeric repeats to the ends of chromosomes (Meyerson *et al*, 1997; Nakamura *et al*, 1997). The differential expression of telomerase in most malignant cells makes it an attractive target for cancer therapy (Mokbel, 2003; Shay and Wright, 2003); however, recent progress in studies on telomerase regulation has shown that telomerase activation is achieved by a process involving various steps including transcriptional and post-transcriptional levels of hTERT gene (Kyo and Inoue, 2002). An alternate splicing of hTERT transcript is one of the regulatory mechanisms of telomerase activity (Ulaner *et al*, 1998). Several alternatively spliced variants of hTERT have been identified (Kilian *et al*, 1997; Ulaner *et al*, 1998; Wick *et al*, 1999; Yi *et al*, 2001); one deletion site induces the α-deletion variant, lacking 36 bp from exon 6, and the other induces the β-deletion variant, lacking 182 bp from exons 7 and 8 (Yi *et al*, 2001). More recently, we have found a new alternatively spliced form, namely the γ-deletion variant, lacking the entire exon 11 (Hisatomi *et al*, 2003; Nagao *et al*, 2004). Since splicing variants are considered to be nonfunctional forms, it is important to discriminate the full-length isoform from variants (Yi *et al*, 2001).

*Correspondence: Dr JH Ohyashiki; E-mail: junko@hh.iij4u.or.jp
Received 4 October 2004; revised 27 January 2005; accepted 4 March 2005; published online 12 April 2005

Another essential element to control telomerase activity is the RNA component of telomerase (hTR: human telomerase template RNA) (Feng *et al*, 1995; Weinrich *et al*, 1997). Several lines of evidence suggest the possibility that reprogramming of telomerase by expression of mutant telomerase RNA would result in impaired function of telomeres (Marusic *et al*, 1997). Indeed, germline mutation *hTR* has been found in the autosomal dominant form of congenital dyskeratosis (DKC) showing progressive telomere shortening without functional telomerase activity (Mitchell *et al*, 1999; Vulliamy *et al*, 2001). More recently, it has been shown that heterozygous telomerase RNA mutations found in DKC and aplastic anaemia reduce telomerase activity via haploinsufficiency (Marrone *et al*, 2004).

The aim of this study was therefore to clarify the quantitative relationship between functionally active telomerase and its components hTR and hTERT (and its spliced variants) using a rapid and highly specific real-time quantitative polymerase chain reaction (RT-Q-PCR) and gain greater insight into the complex regulatory system of telomerase in acute leukaemia cells.

MATERIALS AND METHODS

Patients and cells

We examined 38 consecutive patients with *de novo* acute leukaemia whose peripheral blood or bone marrow cells contained

more than 90% blasts at diagnosis (8–68 years of age): 13 with ALL-L2 and 25 with AML (M1, 6; M2, 14; M3, 2; M4, 2; and M5, 1). *De novo* acute leukaemia was diagnosed according to the French–American–British criteria. All of the ALL patients had precursor B-cell phenotype, and no patient with T-cell ALL was included in this study. Some of the clinical and molecular biological data concerning these patients were reported elsewhere (Ohyashiki *et al*, 2001, 2002). All the samples of peripheral blood or bone marrow cells were separated using a Ficoll–Hypaque gradient, then cell pellets were immediately stored at −80°C. All samples were acquired after obtaining written informed consent from the patients.

Quantification of telomerase activity

Telomerase activity was assessed by TRAP assay according to the method of Kim *et al* and Piatyszak *et al* with minor modifications, using an automated DNA sequencer (Ohyashiki *et al*, 1997). For standardisation of telomerase activity, we used 10 ag of ITAS/telomerase assay and the level of telomerase activity was arbitrary expressed as the ratio of the TRAP ladder/ITAS per microgram of protein as reported previously (Ohyashiki *et al*, 1997).

Real-time reverse transcriptase–polymerase chain reaction of hTERT mRNA and hTR RNA

Total RNA was extracted using the RNeasy Mini Kit (Qiagen, MD, USA). Total RNA (1 μg) was used for cDNA synthesis using a Ready-To-Go You-Prime First-Strand Beads (Amersham Biosciences, Piscataway, NJ, USA) and a pd(N)6 Random Hexamer (Amersham Biosciences). Genomic organisation of the hTERT gene and the location of Taqman primer–probe sets are shown in Figure 1. We designed primers and probes to amplify specially only one form of hTERT (Table 1). Primers and probe sets for hTR are also described in Table 1. In order to generate a standard curve, we constructed plasmids that contain each amplified fragment using a pT7Blue T vector-2 kit (Novagen, Darmstadt, Germany). The Taqman β-actin kit (Applied Biosystems, Foster City, CA, USA) was also used for normalisation of the amount of cDNA used in each PCR. The resulting cDNA (4 μl) was used in each RT–PCR, and then analysed by a 7000 Sequence Detection System (Applied Biosystems). For Taqman assay, a 50 μl of PCR sample contained Taqman universal master mix (Applied Biosystems, Foster City, CA, USA), 3 pmol of each primer pairs and 5 pmol of the corresponding probes were used as recommended by the manufacturer. The PCR conditions were 95°C for 10 min, followed by 55 cycles of 95°C 10 s and 60°C for 1 min. A serial dilution of plasmids was used in each PCR cycle in separate tubes and served as a standard curve. The amount of gene expression in each sample was then expressed as copy numbers per microgram of RNA with respect to the standard curve.

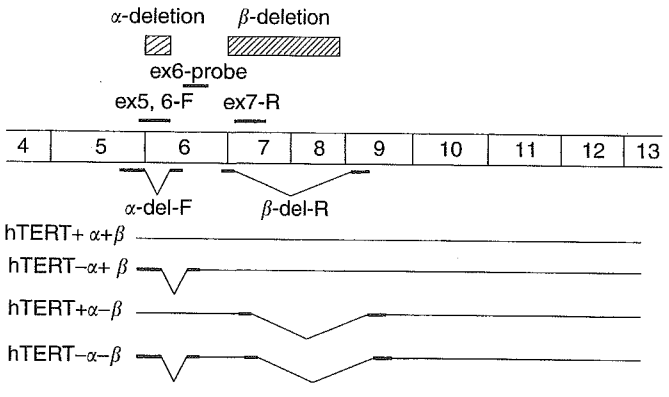

Figure 1 The genomic organisation of the *hTERT* gene and the location of Taqman primer–probe sets. To quantify potentially active full-length hTERT ($+\alpha+\beta$), we used an ex6-F primer and ex7-R primer. We used an α-del-F primer and ex7-R primer for a spliced variant of hTERT$-\alpha+\beta$, and an ex-6F primer and β-del-R primer for the spliced variant of hTERT $+\alpha-\beta$, and an α-del-F primer and β-del-R primer for hTERT$-\alpha-\beta$. For all types of hTERT mRNA, we uniformly used an ex6 probe. The α site causes a 30-base deletion resulting in a no-frameshift mutation, and the β splice site results in a 182-base deletion resulting in a nonsense mutation. The size of the PCR product produced by each primer set depends upon the alternative splicing of the hTERT transcript in the sample.

Table 1 Primers and probes for quantification of the hTERT mRNA and hTR RNA

hTERT	
Ex5, 6-F primer	5′-GAG CTG TAC TTT GTC AAG GTG GGA TG-3′
α-Del-F primer	5′-CTG AGC TGT ACT TTG TCA AGG ACA GG-3′
Ex7-R primer	5′-GGC TGG AGG TCT GTC AAG GTA GAG A-3′
β-Del-R primer	5′-GCA CTG GAC GTA GGA CGT GGC T-3′
Ex6 probe	5′-FAM-CAACCCCAGAACACGTACTGCGTGCGT-3′
hTR	
hTR-F primer	5′-CGC TGT TTT TCT CGC TGA CTT-3′
hTR-R primer	5′-TGC TCT AGA ATG AAG GGT GGA A-3′
hTR probe	5′-FAM-CAG CGG GCG GAA GGA CCT CG-3′

hTR = human telomerase template RNA; FAM = 5-carboxyfluorescein; hTERT = human telomerase reverse transcriptase. To generate full-length hTERT+α+β, ex5, 6-F primer and ex-7-R primer were used. To generate splicing forms of hTERT, we used the following primer sets: hTERT+α−β; ex5, 6-F and α-del-R primers, hTERT−α+β; α-del-F and ex7-R primers, hTERT−α−β; α-del-F and β-del-R primers. The ex6 probe was used to detect full-lengh hTERT+α+β as well as splicing forms of hTERT.

Mutation analysis of *hTR*

PCR-direct sequencing was carried out in order to exclude mutation of the *hTR* gene (NT_005612.14). We designed two pairs of primers to detect mutation of the *hTR* gene: hTR-1F (7597157–7598138), 5′-CTCATGGCCGGAAATGGAAC and hTR-1R (7597633–7597652), 5′-TCTTCCTGCGGCCTGAAAGG; amd hTR-2F (7597864-7597842), 5′-GCCTTCCACCGTTCATTCTAGAG, and hTR-2R (7597413–7597432), 5′-TTTGGAGGTGCCTTCA CGTC. The PCR conditions were as follows: preheating at 95°C for 10 min, followed by 40 cycles 95°C for 30 s, 64°C for 30 s and 72°C for 1 min, and a final extension 72°C for 10 min. Reactions for direct sequencing of the PCR product were performed with BigDye Terminator ver3.1 (Perkin-Elmer Cetus, Freemont, CA, USA).

Statistical analysis

Analysis of variance (one-way ANOVA), correlation analysis, linear regression, Student's *t*-test and the Mann–Whitney *U*-test were calculated using StatView (Brain Power Inc., Calabasas, CA, USA) software for the Macintosh personal computer. Values of $P<0.05$ indicate a statistically significant difference.

RESULTS

Validation of quantification system of hTERT, its spliced forms and hTR

Taqman RT–PCR was validated using a plasmid that contained the target sequence of full-length hTERT $+\alpha+\beta$. There was a linear correlation of full-length hTERT $+\alpha+\beta$ mRNA between 10^1 and 10^6 molecules. Similarly, a linear correlation was observed in each splicing form of hTERT and hTR (data not shown).

Functionally active telomerase is associated with full-length hTERT expression, but did not correlate with hTR expression

In acute leukaemia cells, the relative telomerase activity measured by TRAP assay is associated with the expression level of full-length hTERT $+\alpha+\beta$ mRNA ($P=0.0024$) (Figure 2A). In contrast, there was no correlation between telomerase activity and hTR expression ($P=0.6753$) (Figure 2B). Of note is that there are some exceptional cases showing low telomerase activity despite high copy numbers of hTERT $+\alpha+\beta$ (Figure 2A, arrow). We also found two cases of AML showing high telomerase activity with detectable but low copy numbers of hTERT $+\alpha+\beta$ (Figure 2A, arrowhead).

There is some overlap between telomerase activity in leukaemia cells and that in normal blood cells; therefore, we arbitrarily separated acute leukaemia patients into two groups according to the relative telomerase activity as reported previously (Ohyashiki *et al*, 1997): one with high telomerase activity, equivalent to immortal cells, relative telomerase value greater than 30 (Group-H), and the other with low to moderate telomerase activity (Group-L). The hTERT expression level is significantly high in Group-H ($P=0.0013$) (Figure 3A), while association between telomerase activity and hTR expression was not significant (Figure 3B). This indicates that functionally active telomerase activity is generally associated with hTERT expression, but in some cases the TERT expression does not simply reflect the enzymatic activity.

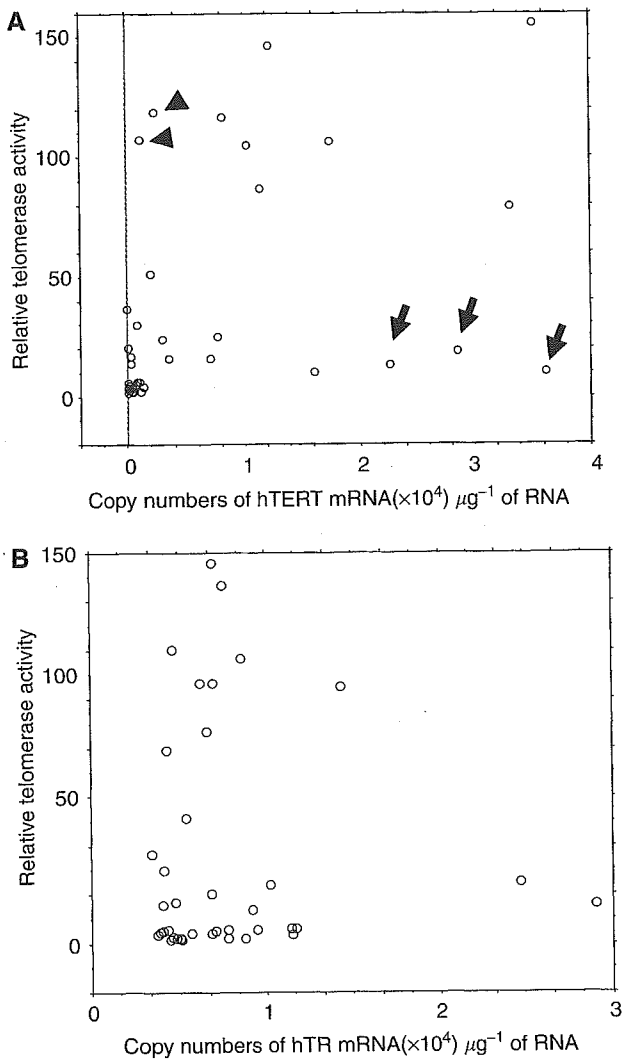

Figure 2 Relationship between telomerase activity level and hTERT $+\alpha+\beta$ mRNA expression level (**A**) and telomerase activity level and hTR RNA expression level (**B**). The level of telomerase activity was generally associated with the copy numbers of full-length hTERT mRNA, but there were some exceptional cases showing low telomerase activity despite high copy numbers of hTERT $+\alpha+\beta$ (arrow) and cases showing high telomerase activity with detectable but low copy numbers of hTERT $+\alpha+\beta$ (arrowhead).

Ratio of hTR and hTERT is critical to determine enzymatic activity of telomerase

To address the question as to why some patients show low telomerase activity despite high hTERT $+\alpha+\beta$ expression, we next compared the ratio of hTR and hTERT. The Group-L patients

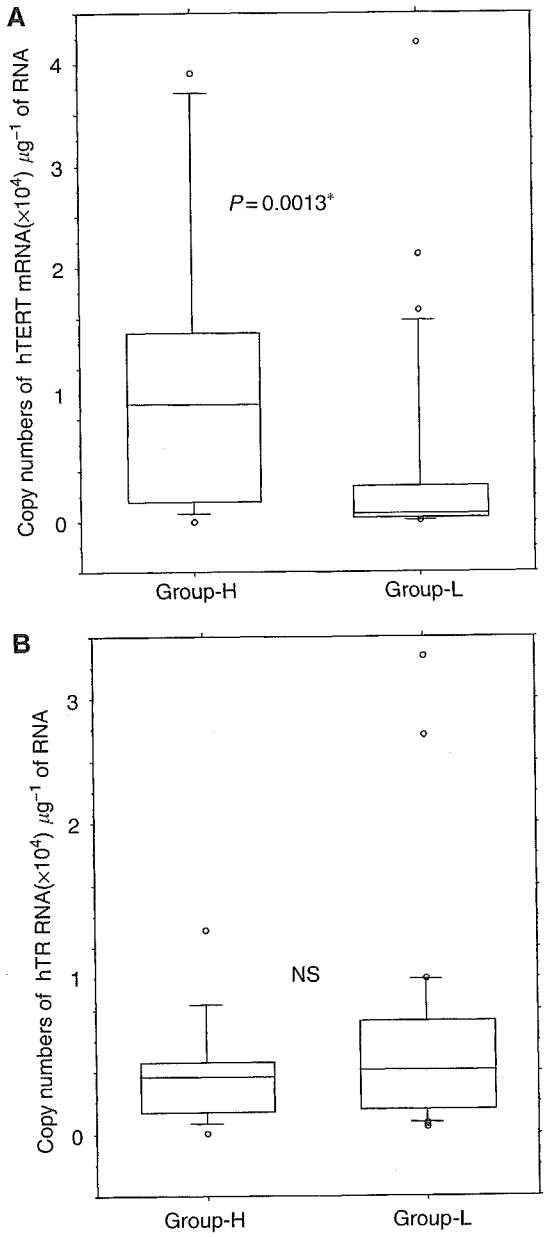

Figure 3 Expression level of hTERT (**A**) and hTR (**B**) in acute leukaemia patients. Group-H: Patients with high telomerase activity; group-L: patients with low–moderate telomerase activity. Expression level of hTERT is significantly higher in Group-H, but there was no difference of hTR expression level in the two groups.

showed significantly lower copy numbers of hTR ($P=0.0284$), and the hTR/hTERT ratio was significantly lower than those in Group-H patients ($P=0.0094$) (Figure 4). This indicates the possibility that the combination of full-length hTERT and hTR is necessary to create a functionally active telomerase activity in leukaemia cells *in vivo*. The quantitative relationships between functionally active telomerase activity and its components are shown in Figure 5. There was an obvious difference between patients with low telomerase activity, despite high full-length hTERT expression (UPN41, 40 and 44, Figure 5A–C, respectively) and patients with high telomerase activity (UPN15, Figure 5D). We next analysed the mutation of the *hTR* gene in three patients showing a marked discrepancy between hTERT $+\alpha+\beta$ expression and telomerase activity, in order to determine whether this phenomenon is related to mutation of *hTR*. No case showed mutation of *hTR* gene within the limit of our primers. This indicates that the discrepancy between expression of full-length hTERT and functionally active telomerase activity is possibly due to the quantity of hTR but not to the gene structure of *hTR*.

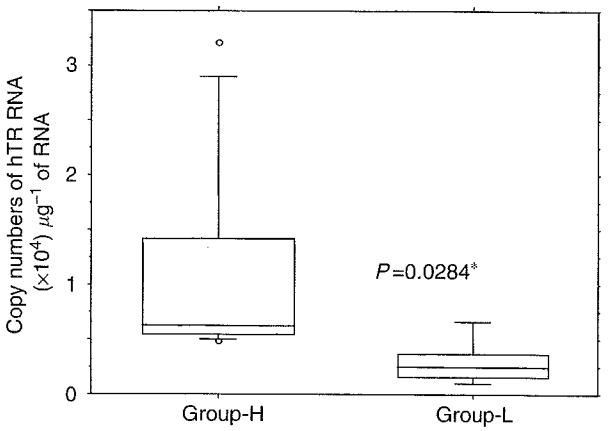

Figure 4 Expression level of hTR in patients with high hTERT mRNA expression. Group-H: Patients with high telomerase activity; group-L: patients with low–moderate telomerase activity. The expression level of hTR is significantly lower in Group-L.

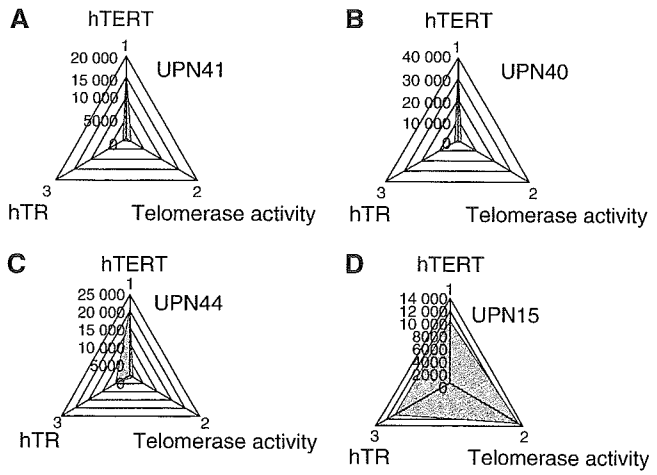

Figure 5 The quantitative relationship between functionally active telomerase activity and its components. Shapes of three elements (full-length hTERT, hTR and relative telomerase activity) are different in patients with low telomerase activity despite high full-length hTERT expression (**A**–**C**) and that in a patient with high telomerase activity (**D**).

Role of nonactive splicing forms of hTERT

To clarify whether the splicing mechanism of hTERT really affects the level of functional telomerase activity or not, we next compared the expression level of hTERT $+\alpha+\beta$ and three spliced forms of hTERT. The expression level of full-length hTERT $+\alpha+\beta$ mRNA was generally associated with levels of spliced variants hTERT $+\alpha-\beta$ ($P=0.0434$) (Figure 6B) and hTERT $-\alpha-\beta$ ($P=0.0084$) (Figure 6C), while the relationship between the expression level of full-length hTERT $+\alpha+\beta$ mRNA and those of spliced variant hTERT $-\alpha+\beta$ was not statistically significant ($P=0.1109$) (Figure 6A). The ratio of spliced form/full-length hTERT $+\alpha+\beta$ mRNA varied, but tended to be higher in Group-L patients compared to those in Group-H, although the difference was not always statistically significant: hTERT $+\alpha-\beta$/full-length hTERT $+\alpha+\beta$($P=0.101$),hTERT $-\alpha+\beta$/full-lengthhTERT $+\alpha+\beta$ ($P=0.048$) (Figure 6D) and hTERT $-\alpha-\beta$/full-length hTERT $+\alpha+\beta$ ($P=0.201$). This indicates that increase of nonfunctional splicing form of hTERT may play some role in telomerase downregulation.

DISCUSSION

Telomerase and telomere length are two important markers that are rapidly gaining importance as targets for cures of several age-related diseases including cancer. We therefore sought to determine whether therapeutic approaches to leukaemia targeting telomerase should consider the quantitative relationship between telomerase and its components or not. Acute leukaemia is composed of a heterogeneous population in terms of cell lineage, cell differentiation and proliferative potential. In the current study, the level of telomerase activity and telomerase components revealed considerable patient-to-patient variation; however, we found telomerase activity is significantly associated with hTERT expression in most patients but did not correlate with hTR expression. We also found that in some cases telomerase activity was low, despite high copy numbers of full-length hTERT mRNA correlating with low copy numbers of hTR. This is of particular interest given that hTR has now been shown to be limiting for telomere homeostasis *in vivo*, as seen in DKC (Mitchell *et al*, 1999; Vulliamy *et al*, 2001).

Recently, mutations of *hTR* have been reported in a subset of aplastic anaemia (Vulliamy *et al*, 2002). Although it is still controversial whether the genetic change of *hTR* sequence is polymorphism or not (Wilson *et al*, 2003; Yamaguchi *et al*, 2003), Ly *et al* (2003) demonstrated that naturally occurring *hTR* sequence mutation polymorphism in such patients can inhibit telomerase activity by disrupting critical structures within the *hTR* core domain. Unlike DKC, neither mutation nor deletion of *hTR* was detected in this study by direct sequencing. This suggests that the amount of hTR is so low that as a result there is an excess of unbound hTERT mRNA. Indeed, the expression level of hTR is consistent in leukaemia cell lines showing high telomerase activity (Yi *et al*, 2001). The mechanism of telomerase regulation in acute leukaemia cell is likely to be different from those in DKC and bone marrow failure syndrome; however, the ratio of hTR and hTERT might play an important role to contribute functionally active telomerase activity and telomere homeostasis *in vivo*, whether or not mutated *hTR* affect telomerase activity via haploinsufficiency.

In the current study, we found two exceptional cases with high telomerase activity despite low expression of hTERT; therefore, we could not completely rule out the possibility that hTERT-associated proteins such as heat-shock proteins may affect the activity of the telomerase holoenzyme.

Alternative splicing machinery of hTERT is considered to be tissue specific and to influence telomere lengths during human development (Ulaner *et al*, 2001). It has been shown that hTERT RNA alternative splicing mediates telomerase downregulation induced by the G-quadruplex ligand 12459 (Gomez *et al*, 2004).

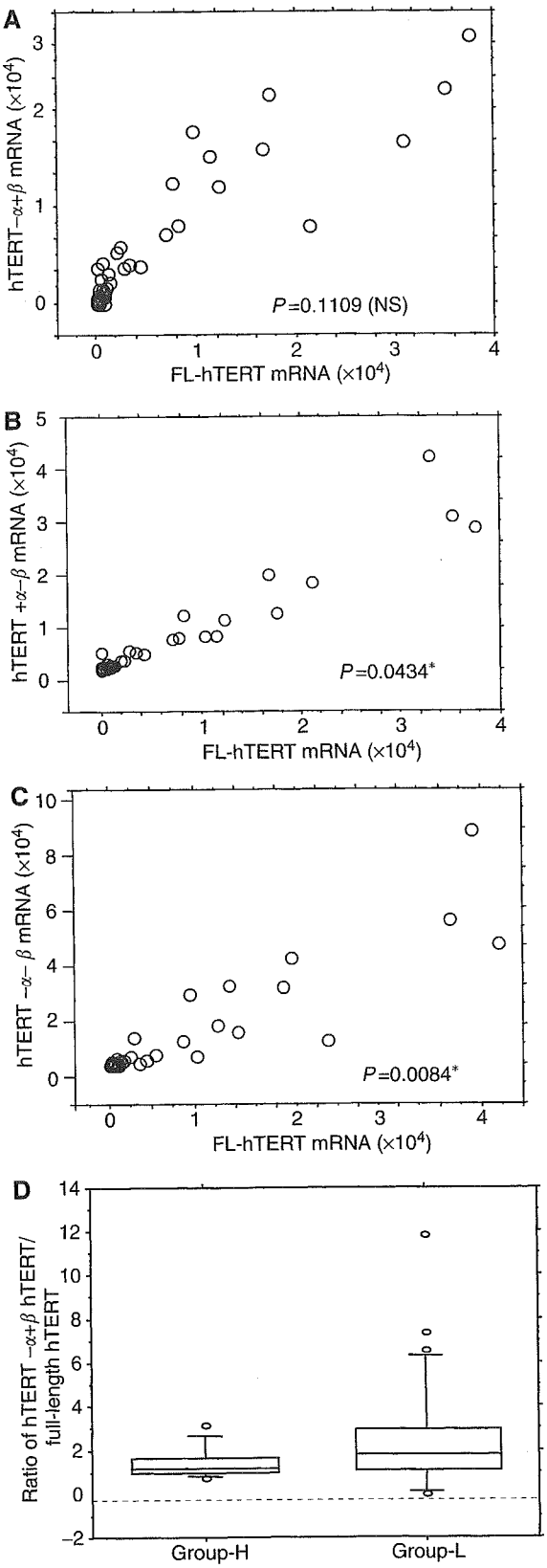

Figure 6 Relationship between hTERT + α + β mRNA expression level and its spliced forms (**A**: hTERT−α + β (**B**) hTERT + α−β (**C**) hTERT−α−β). The ratio of hTERT−α + β/hTERT + α + β mRNA (full-length hTERT) is significantly lower in Group-H (**D**) ($P = 0.048$).

However, the ratios of spliced nonactive forms and full-length hTERT in primary acute leukaemia cells are highly varied. Of note is that the ratio of splicing variants and full-length hTERT is lower in patients with high telomerase activity ($n = 7$) than that in patients without high telomerase activity ($n = 31$). It is known that splicing variants lack the α site function as a dominant-negative inhibitor of telomerase (Colgin *et al*, 2000; Yi *et al*, 2001). Although we could not show direct evidence that the spliced inactive variant of hTERT downregulates full-length wild-type hTERT, it is likely that splicing variant mRNA is related with some regulatory mechanism in acute leukaemia cells without exhibiting high telomerase activity. While, the meaning of these epiphenomena is still uncertain, the regulatory mechanism of telomerase in leukaemia cells with low telomerase activity appears to be similar to that in normal counter parts. Zaffaroni *et al* (2002) reported that alternative splicing mechanisms of hTERT that regulate telomerase activity in normal tissue might be lost during malignant transformation in breast tumours. Taken together with Zaffaroni's observation (2002), our results suggest that acute leukaemia cells with high telomerase activity might lose their regulatory mechanism during disease progression.

Our findings suggest that the regulatory mechanisms in leukaemia cells may be heterogeneous; therefore, the therapeutic approach targeting telomerase should be considered based on the quantitative relationship between telomerase and its components. While the number of patients studied in the current study is limited, our results suggest the necessity, and provide the basis, for more detailed studies on the complex regulatory mechanism of telomerase activity in haematologic neoplasia that may lead to the development of new cancer therapeutic strategies.

ACKNOWLEDGEMENTS

We are indebted to Professor J Patrick Barron of the International Medical Communications Center of Tokyo Medical University for his review of this paper. Thanks are also due to Professor Jerry W Shay of The University of Texas Southwestern Medical Center for his helpful suggestions. This work was supported by 'High-Tech Research Center' Project for private universities: matching fund subsidy from the MEXT (Ministry of Education, Culture, Sports, Science and Technology, 2003–2007), and by the 'University-Industry Joint Research Project' for private universities: matching fund subsidy from the MEXT, 2002–2006.

REFERENCES

Colgin LM, Wilkinson C, Englezou A, Kilian A, Robinson MO, Reddel RR (2000) The hTERT alpha splice variant is a dominant negative inhibitor of telomerase activity. *Neoplasia* **2:** 426–432

Feng J, Funk WD, Wang SS, Weinrich SL, Avilion AA, Chiu CP, Adams RR, Chang E, Allsopp RC, Yu J, Le S, West MD, Harley CB, Andrews WH, Greider CW, Villeponteau B (1995) The RNA component of human telomerase. *Science* **269:** 1236–1241

Gomez D, Lemarteleur T, Lacroix L, Mailliet P, Mergny J-L, Riou F (2004) Telomere downregulation induced by the G-quadroplex ligand 12459 in A 549 cells id medicated by hTERT RNA alternative splicing. *Nucleic Acid Res* **32:** 371–379

Hisatomi H, Ohyashiki K, Ohyashiki JH, Nagao K, Kanamaru T, Hirata H, Hibi N, Tsukada Y (2003) Expression profile of a gamma-deletion variant of the human telomerase reverse transcriptase gene. *Neoplasia* **5:** 193–197

Kilian A, Bowtell DD, Abud HE, Hime GR, Venter DJ, Keese PK, Duncan EL, Reddel RR, Jefferson RA (1997) Isolation of a candidate human telomerase catalytic subunit gene, which reveals complex splicing patterns in different cell types. *Hum Mol Genet* **6:** 2011–2019

Kyo S, Inoue M (2002) Complex regulatory mechanisms of telomerase activity in normal and cancer cells: how can we apply them for cancer therapy? *Oncongene* **21:** 688–697

Ly H, Blackburn EH, Parslow TG (2003) Comprehensive structure–function analysis of the core domain of human telomerase RNA. *Mol Cell Biol* **23:** 6849–6856

Marrone A, Stevens D, Vulliamy T, Dokal I, Mason PJ (2004) Heterozygous telomerase RNA mutations found in dyskeratosis congenital and aplastic anemia reduce telomerase activity via haploinsufficiency. *Blood*, prepublished on line August 19

Marusic L, Anton M, Tidy A, Wang P, Villeponteau B, Bacchetti S (1997) Reprogramming of telomerase by expression of mutant telomerase RNA template in human cells leads to altered telomeres that correlate with reduced cell viability. *Mol Cell Biol* **17:** 6394–6401

Meyerson M, Counter CM, Eaton EN, Ellison LW, Steiner P, Caddle SD, Ziaugra L, Beijersbergen RL, Davidorff MJ, Liu Q, Bacchetti S, Haber DA, Weinberg RA (1997) hEST2, the putative human telomerase catalytic subunit gene, is up-regulated in tumor cells and during immortalization. *Cell* **90:** 785–795

Mitchell JR, Wood E, Collins K (1999) A telomerase component is defective in the human disease dyskeratosis congenita. *Nature* **402:** 551–555

Mokbel K (2003) The evolving role of telomerase inhibitors in the treatment of cancer. *Curr Med Res Opin* **19:** 470–472

Nagao K, Katsumata K, Aizawa Y, Saito N, Hirata H, Sasaki H, Yamamoto S, Hikiji K, Koiwa T, Hisatomi H (2004) Differential alternative splicing expressions of telomerase reverse transcriptase in gastrointestinal cell lines. *Oncol Rep* **11:** 127–131

Nakamura TM, morin GB, Chapman KB, Weinrich SL, Andrews WH, Lingner J, Harley CB, Cech TR (1997) Telomerase catalytic subunit homologs from fission yeast and human. *Science* **277:** 955–959

Ohyashiki JH, Hayashi S, Yahata N, Iwama H, Ando K, Tauchi T, Ohyashiki K (2001) Impaired telomere regulation mechanism by TRF1 (telomere-binding protein), but not TRF2 expression, in acute leukemia cells. *Int J Oncol* **18:** 593–598

Ohyashiki JH, Ohyashiki K, Iwama H, Hayashi S, Toyama K, Shay JW (1997) Clinical implications of telomerase activity levels in acute leukemia. *Clin Cancer Res* **3:** 619–625

Ohyashiki JH, Sashida G, Tauchi T, Ohyashiki K (2002) Telomeres and telomerase in hematologic neoplasia. *Oncogene* **21:** 680–687

Shay JW, Wright WE (2003) Telomerase: a target for cancer therapeutics. *Cancer Cell* **2:** 257–265

Ulaner GA, Hu JF, Vu TH, Giudice LC, Hoffman AR (2001) Tissue-specific alternate splicing of human telomerase reverse transcriptase (hTERT) influences telomere lengths during human development. *Int J Cancer* **91:** 644–649

Ulaner GA, Hu JF, Vu TH, Giudice LC, Hoffman AR (1998) Telomerase activity in human development is regulated by human telomerase reverse transcriptase (hTERT) transcription and by alternate splicing of hTERT transcripts. *Cancer Res* **58:** 4168–4172

Vulliamy T, Marrone A, Dokal I, Mason PJ (2002) Association between aplastic anaemia and mutations in telomerase RNA. *Lancet* **359:** 2168–2170

Vulliamy T, Marrone A, Goldman F, Dearlove A, Bessler M, Mason PJ, Dokal I (2001) The RNA component of telomerase is mutated in autosomal dominant dyskeratosis congenita. *Nature* **413:** 432–435

Weinrich SL, Pruzan R, Ma L, Ouellette M, Tesmer VM, Holt SE, Bodnar AG, Lichtsteiner S, Kim NW, Trager JB, Taylor RD, Carlos R, Andrews WH, Wright WE, Shay JW, Harley CB, Morin GB (1997) Reconstitution of human telomerase with the template RNA component hTR and the catalytic protein subunit hTRT. *Nat Genet* **17:** 498–502

Wick M, Zubov D, Hagen G (1999) Genomic organization and promoter characterization of the gene encoding the human telomerase reverse transcriptase (hTERT). *Gene* **17:** 97–106

Wilson DB, Ivanovich J, Whelan A, Goodfellow PJ, Bessler M (2003) Human telomerase RNA mutations and bone marrow failure. *Lancet* **361:** 1993–1994

Yamaguchi H, Baerlocher GM, Lansdorp PM, Chanock SJ, Nunez O, Sloand E, Young NS (2003) Mutations of the human telomerase RNA gene (TERC) in aplastic anemia and myelodysplastic syndrome. *Blood* **102:** 916–918

Yi X, Shay JW, Wright WE (2001) Quantification of telomerase components and hTERT mRNA splicing patterns in immortal human cells. *Nucleic Acid Res* **29:** 4825–4919

Zaffaroni N, Della Porta C, Villa R, Botti C, Buglioni S, Mottolese M, Grazia A, Daidone M (2002) Transcription and alternative splicing of telomerase reverse transcriptase in benign and malignant breast tumours and in adjacent mammary glandular tissues: implications for telomerase activity. *J Pathol* **198:** 37–46

TEF, an antiapoptotic bZIP transcription factor related to the oncogenic E2A-HLF chimera, inhibits cell growth by down-regulating expression of the common β chain of cytokine receptors

Takeshi Inukai, Toshiya Inaba, Jinjun Dang, Ryoko Kuribara, Keiya Ozawa, Atsushi Miyajima, Wenshu Wu, A. Thomas Look, Yojiro Arinobu, Hiromi Iwasaki, Koichi Akashi, Keiko Kagami, Kumiko Goi, Kanji Sugita, and Shinpei Nakazawa

Gain and/or loss of function mediated by chimeric transcription factors generated by nonrandom translocations in leukemia is a key to understanding oncogenesis. E2A–hepatic leukemia factor (HLF), a chimeric basic region/leucine zipper (bZIP) transcription factor expressed in t(17;19)–positive leukemia cells, contributes to leukemogenesis through its potential to inhibit apoptosis. To identify physiologic counterparts of this chimera, we investigated the function of other bZIP factors that bind to the same DNA sequence recognized by E2A-HLF. Here, we show that thyrotroph embryonic factor (TEF), which shares a high level of sequence identity with HLF and recognizes the same DNA sequence, is expressed in a small fraction of each subset of hematolymphoid progenitors. When TEF was introduced into FL5.12 interleukin 3 (IL-3)–dependent cells, TEF protected the cells from apoptosis due to IL-3 deprivation. Unexpectedly, TEF also almost completely down-regulated expression of the common β (βc) chain of cytokine receptors. Consequently, TEF-expressing cells accumulated in G_0/G_1 phase without undergoing apoptosis. These findings suggest that TEF is one of the apoptotic regulators in hematopoietic progenitors and controls hematopoietic-cell proliferation by regulating the expression of the βc chain. In contrast, E2A-HLF promoted cell survival more efficiently than TEF but did not down-regulate βc chain expression, suggesting that E2A-HLF retains ideal properties for driving leukemic transformation. (Blood. 2005;105:4437-4444)

Introduction

Since key systems that regulate cell survival have been conserved through evolution, relatively simple organisms such as *Caenorhabditis elegans* often provide insight into the complex mechanisms that control cell fate in mammals.[1] The genetic approach demonstrated that 2 factors, cell death specification protein 1 (CES-1) and CES-2, regulate the programmed cell death of serotonergic neurosecretory motor (NSM) neurons in *C elegans* in a cell type–specific fashion.[2] Further studies revealed that CES-2 is a transcription factor that belongs to the basic region/leucine zipper (bZIP) superfamily (Figure 1).[3] CES-2 negatively regulates CES-1, a member of the snail family of zinc finger transcription factors,[4] and CES-1 appears to determine the fate of NSM sisters by negatively regulating the expression of *egl1*, a BH3-only proapoptotic member of the B cell lymphoma (Bcl-2) superfamily.[5-7]

Transcription factors that bind to the DNA sequence elements recognized by CES-2 might play important roles in cell type–specific cell death in mammals. The E2A–hepatic leukemia factor (HLF) fusion transcription factor is a good example. This chimera is derived from childhood acute pro-B-cell leukemia harboring a t(17;19) chromosomal translocation.[8-10] It contains the transactivation domains of E2A and the bZIP DNA-binding and dimerization domain of HLF (Figure 1). E2A-HLF promotes the anchorage-independent growth of murine fibroblasts as a homodimer that depends on both the transactivation domain of E2A and the bZIP domain of HLF.[11,12] E2A-HLF induces the expression of annexin II,[13] annexin V, and sushi-repeat protein upregulated in leukemia (SRPUL),[14] which have been postulated to play paraneoplastic roles in coagulopathies and bone invasion, as well as groucho-related genes, and E2A-HLF also suppresses Runt-related 1 (RUNX1).[15] In addition, we and others established transgenic mice expressing *E2AHLF* that develop T-lineage lymphoid malignancies.[16,17] Of note, we demonstrated that E2A-HLF binds avidly to the sequence recognized by CES-2 and protects cells from apoptosis due to growth factor deprivation without promoting cell proliferation.[18-20] The close homology between the bZIP domains of HLF and CES-2 suggests that E2A-HLF subverts a cell-death pathway through a mechanism similar to that used by CES-2 in the worm. Indeed, we have identified SLUG, a zinc finger transcription factor closely related to CES-1, as one of the downstream targets of E2A-HLF in human leukemias associated with the 17;19 translocation and found that SLUG has antiapoptotic potential.[21,22]

These findings suggest that a cell-death pathway in mammalian hematopoietic cells is normally regulated by bZIP factors that exhibit a DNA-binding specificity similar to that of CES-2 or E2A-HLF. HLF is obviously a good candidate for the regulator of apoptosis in hematopoiesis; however, HLF is not expressed in

From the Department of Pediatrics, School of Medicine, University of Yamanashi, Yamanashi, Japan; Department of Molecular Oncology, Research Institute for Radiation Biology and Medicine, Hiroshima University, Hiroshima, Japan; Department of Experimental Oncology, St Jude Children's Research Hospital, Memphis, TN; Division of Hematology, Jichi Medical School, Tochigi, Japan; Institute of Molecular and Cellular Bioscience, the University of Tokyo, Tokyo, Japan; Pediatric Oncology Department and Department of Cancer Immunology & AIDS, Dana-Farber Cancer Institute, Boston, MA.

Submitted August 2, 2004; accepted January 2, 2005. Prepublished online as *Blood* First Edition Paper, January 21, 2005; DOI 10.1182/blood-2004-08-2976.

Reprints: Takeshi Inukai, Department of Pediatrics, School of Medicine, University of Yamanashi, 1110 Shimokato, Tamaho-cho, Nakakoma-gun, Yamanashi 409-3898, Japan. e-mail: tinukai@yamanashi.ac.jp

The publication costs of this article were defrayed in part by page charge payment. Therefore, and solely to indicate this fact, this article is hereby marked "advertisement" in accordance with 18 U.S.C. section 1734.

hematopoietic progenitors and, moreover, enforced expression of HLF in cytokine-dependent cells failed to inhibit apoptosis.[18,19] We then identified a bZIP factor, E4 promoter binding protein (E4BP4)/nuclear factor regulated by IL-3 (NFIL3) (Figure 1), as a physiologic counterpart of E2A-HLF. E4BP4 has nearly identical DNA-binding specificity to CES-2 and its expression is tightly regulated by interleukin (IL-3) in IL-3–dependent cell lines such as FL5.12 and Baf-3. Moreover, enforced expression of E4BP4 delays apoptosis of IL-3–deprived cells.[23,24] These data suggested that subversion of the roles of antiapoptotic bZIP factors normally regulated by cytokines is 1 critical aspect of leukemogenesis induced by E2A-HLF.

Other bZIP factors may also play important roles in the regulation of hematopoietic cell survival. HLF is a member of the proline- and acidic amino acid–rich (PAR) bZIP family, which also includes thyrotroph embryonic factor (TEF)[25] and albumin promoter D-box–binding protein (DBP)[26] (Figure 1). TEF was originally cloned as a factor expressed in the developing anterior pituitary gland that could *trans*-activate the *TSHβ* promoter,[25] whereas DBP was cloned as a liver-enriched transcriptional activator that binds to the D element of the albumin promoter.[26] It has been well documented that the PAR proteins as well as E4BP4 are implicated in circadian control.[27-33] PAR proteins may also be involved in the regulation of cell death because all 3 PAR proteins exhibit nearly identical DNA-binding specificity to that of E4BP4 and CES-2.[25,26,28,29,34-37] Here we demonstrate that TEF promotes the survival of FL5.12 cells due to IL-3 starvation. Unexpectedly, we also found that TEF potently represses the expression of the β subunits of the IL-3 receptor, blocking proliferation and leading to arrest of the cell cycle in the G_0/G_1 phase, even in the presence of IL-3.

Materials and methods

Constructs of eukaryotic expression vectors

Expression plasmids containing the cDNAs of wild-type *TEF* (pMT-TEF), a mutated *TEF* (pMT-TEF basic mutant [BX]), and *E2AHLF* (pMT–E2A-HLF) were constructed with the pMT-CB6$^+$ eukaryotic expression vector (a gift from F. Rauscher III, Wistar Institute, Philadelphia, PA), which contains the inserted cDNA under the control of a sheep metallothionein promoter as well as the neomycin resistance gene driven by the simian virus 40 early promoter. The cDNA encoding a basic mutant of TEF (TEF/BX) that contained substitutions for 6 of the amino acid residues in the basic region critical for DNA binding (TRRKKNNVAAK mutated to TSPKSYNVPPK; single-letter code) was made by polymerase chain reaction (PCR) mutagenesis.

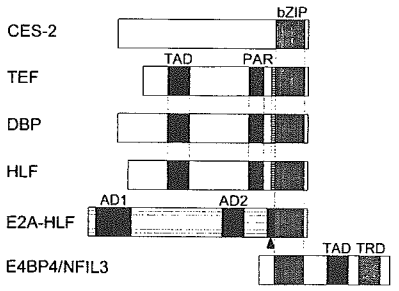

Figure 1. Schematic representation of the CES-2, TEF, DBP, HLF, E2A-HLF, and E4BP4/NFIL3 proteins. The CES-2 protein in *C elegans* contains a basic region/leucine zipper (bZIP) domain in the carboxyl-terminal region and acts as a transrepressor. TEF, DBP, and HLF contain a proline- and acidic amino acid–rich (PAR) domain as well as a bZIP domain in the carboxyl-terminal region, which shows high level of sequence identity to that of CES-2. TEF, DBP, and HLF each also contain a *trans*-activation domain (TAD) and can act as transcriptional activators. The E2A-HLF fusion protein, which is expressed in t(17;19)–positive leukemia cells, retains the 2 transactivation domains in the amino terminal of E2A (AD1 and AD2) but not its basic region/helix-loop-helix domain, which is replaced by the bZIP domain of HLF. E2A-HLF has a joining region (■ with arrowhead) generated at the breakpoint but not the basic region extension (BRE; indicated with ▤) nor the PAR domain of HLF, which contribute to sequence-specific DNA binding. E4BP4/NFIL3 contains a bZIP domain in its amino-terminal region and has nearly identical DNA-binding specificity as that of CES-2, TEF, DBP, HLF, and E2A-HLF. E4BP4 acts as either a transactivator or transrepressor depending on complexes formed by its TAD or transrepression domain (TRD) in its carboxyl-terminal region.

Cell culture and cell survival assay

FL5.12 cells, which are murine IL-3–dependent cells, were cultured in RPMI 1640 medium supplemented with 10% fetal calf serum and 0.5% 10T1/2 cell-conditioned medium as a source of IL-3. Transfectants were generated by electroporation using 2×10^7 cells and 80 μg of DNA with a gene pulser (Bio-Rad, Hercules, CA) set at 300 mV and 960 μF. Cells were then cultured in 24-well dishes and selected in the presence of the neomycin analog G418 (0.6 mg/mL) for 2 weeks. The induction of protein expression with Zn in G418-resistant cells was confirmed by immunoblot analysis. Cell growth and cell survival experiments were performed using 3 independent pools of cells, and the results of representative data of multiple experiments are shown. For cell survival assays, cells growing exponentially in IL-3–containing medium were precultured for 16 hours in the presence or absence of 100 μM $ZnSO_4$. Cells were washed with IL-3–free medium twice and were adjusted to 5×10^5 cells per milliliter. Viable cell counts were determined by trypan blue dye exclusion.

Immunoblot analysis

Cells were solubilized in Nonidet P-40 lysis buffer (150 mM NaCl, 1.0% Nonidet P-40, 50 mM Tris [tris(hydroxymethyl)aminomethane; pH 8.0]), and total cellular proteins were separated by sodium dodecyl sulfate–polyacrylamide gel electrophoresis. After wet electrotransfer onto polyvinylidene difluoride membranes, proteins were detected with the following primary antibodies: anti-HLF c-terminal (C),[35] anti-p44/42 mitogen-activated protein kinase (MAPK; New England BioLabs, Beverly, MA), anti-p70S6K (New England BioLabs), anti-Akt (New England BioLabs), antiphospho–signal transducers and activators of transcription 5 (anti–phospho-STAT5; Tyr694; New England BioLabs), anti–phospho-p44/42MAPK (Thr202/Tyr204; New England BioLabs), anti–phospho-p70S6K (Thr421/Ser424; New England BioLabs), and anti–phospho-Akt (Ser473; New England BioLabs) rabbit serum, or anti–β-tubulin (Pharmingen, San Diego, CA), antiphosphotyrosine (Upstate Biotechnology, Lake Placid, NY), and anti-STAT5 (Transduction Laboratories, Lexington, KY) mouse monoclonal antibodies. Then, the blots were stained by horseradish peroxidase–conjugated anti–rabbit or anti–mouse immunoglobulin G (IgG) and IgM secondary antibodies (MBL, Nagoya, Japan), respectively, and subjected to enhanced chemiluminescence detection (Amersham Life Science, Arlington Heights, IL).

Flow cytometric analysis

Cells (2×10^5) were washed with phosphate-buffered saline (PBS) and incubated with rat monoclonal antibodies specific for the mouse IL-3 receptor α chain (5B11)[38] or the mouse IL-3 receptor β chain (AIC2A; β_{IL3}; 9D3)[39] on ice for 30 minutes. Cells were washed with PBS and stained with a fluorescein isothiocyanate (FITC)–conjugated goat anti–rat IgG (Jackson Immuno Research Laboratories, West Grove, PA). For detection of the common β chain of the IL-3 receptor (AIC2B; β_C), cells were incubated with an anti–mouse β_C chain hamster monoclonal antibody (MBL), followed by incubation with an FITC-conjugated goat anti–hamster IgG secondary antibody (Jackson Immuno Research Laboratories). Cells were analyzed by flow cytometry (FACS Calibar; Becton Dickinson, San Jose, CA).

Northern blot analysis

Total cellular RNA was isolated by the guanidinium-cesium chloride method. RNA samples (approximately 20 μg per lane) were separated by

electrophoresis in 1% agarose gel containing 2.2 M formaldehyde, transferred to nylon membranes, and hybridized with the appropriate probes according to the standard procedure. For Northern blot analysis of multiple human hematolymphoid tissues, the blot was purchased from Clontech (Palo Alto, CA). Unique cDNA probes in the 3′ untranslated region of the PAR genes,[40] a 1.3-kilobase (kb) *Xho*I fragment of mouse IL-3 receptor α-chain cDNA, and a 0.8-kb *Xho*I/*Bam*HI fragment of mouse IL-3 receptor β_{IL3} chain cDNA were used as probes.

Analysis of gene expression in subsets of hematopoietic stem and progenitor cells

Cells (5×10^3) with surface marker expression patterns typical of hematopoietic stem cells (HSCs) and various types of myeloid and lymphoid progenitors were sorted from mouse bone marrow by fluorescence-activated cell sorting (FACS), as previously described.[41] Total RNA was prepared with TRIZOL reagent and subjected to cDNA synthesis with the SuperScript first-strand cDNA synthesis system (GIBCO, Carlsbad, CA). PCR was performed for 40 cycles of 94°C for 30 seconds, 55°C for 45 seconds, and 72°C for 45seconds with the following primers: 5′-ACCATCTTCCTCTACTGCCATCTTTCAG and 5′-GTACTTGGTCTCGTACTTGGACACGATG for first-round PCR; 5′-GTGATCTGGTTCTCCTTCAG for nested PCR amplification of *Tef;* and 5′-CACAGGACTAGAACACCTGC and 5′-GCTGGTGAAAAG-GACCTCT for PCR amplification of *Hprt*.

Electrophoretic mobility shift assay

Binding reactions in electrophoretic mobility shift assay (EMSA) were performed with a ^{32}P–end-labeled DNA oligonucleotide probe (2×10^4 counts per minute [cpm]) in 10 μL of binding buffer (12% glycerol, 12 mM HEPES [*N*-2-hydroxyethylpiperazine-*N*′-2-ethanesulfonic acid, pH 7.9], 4 mM Tris [pH 7.9], 133 mM KCl, 300 mg of bovine serum albumin per milliliter) and 5 μL of nuclear proteins extracted from FL5.12 cells by standard procedures, as previously described.[35,42] The oligonucleotide probes used were wild-type HLF consensus sequence (CS) (5′-GCTA-CATATTACGTAATAAGCGTT-3′); wild-type β-casein for STAT5 (5′-AGATTTCTAGGAATTCAATCC-3′); and mutant β-casein (5′-AGATT-TAGTTTAATTCAATCC-3′). As a carrier DNA, 1.5 μg of sheared calf thymus DNA or poly-d(I)d(C) was added to the reaction mixture testing for binding to HLF-CS or β-casein probe, respectively. The entire mixture was incubated at 30°C for 15 minutes. In the competition inhibition experiments, an approximately 100-fold molar excess of the unlabeled oligonucleotide was added to the reaction mixture. One microliter of polyvalent HLF(C) antiserum or preimmune rabbit serum was added to the nuclear lysates and incubated at 4°C for 30 minutes prior to the DNA-binding reaction. Nondenaturing polyacrylamide gels containing 4% acrylamide and 2.5% glycerol were prerun at 4°C in a high-ionic-strength Tris-glycine buffer for 30 minutes, loaded with the samples containing protein–DNA complexes, run at 35 mA for approximately 90 minutes, dried under vacuum, and analyzed by autoradiography.

Results

Expression of *TEF* in hematolymphoid tissues

The 3 members of the PAR family of proteins are differentially expressed in tissues and organs.[8,10,40] In contrast to HLF, which shows tissue-specific expression, TEF and DBP are expressed ubiquitously, although their expression in normal hematopoietic and lymphoid tissues has not been clarified. First, we performed Northern blot analysis of human hematolymphoid tissues using a specific cDNA probe. As shown in Figure 2A, *TEF* was expressed in the spleen, lymph node, thymus, and fetal liver but was nearly undetectable in peripheral blood leukocytes and bone marrow. *DBP* was widely expressed in hematolymphoid tissues, whereas *HLF* was expressed in the fetal liver alone. Second, subsets of mouse hematolymphoid progenitors were sorted from the bone marrow

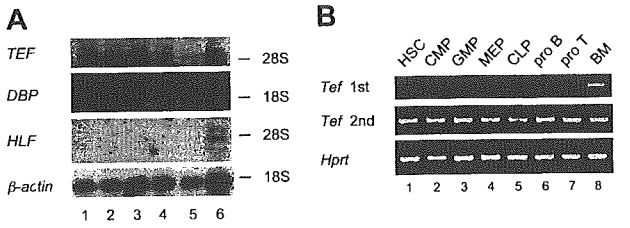

Figure 2. Expression of *TEF* during hematopoiesis. (A) Northern blot analysis of human hematolymphoid tissues. The blot was hybridized with human *TEF, DBP, HLF,* and β-actin cDNA probes. Lane 1, spleen; lane 2, lymph node; lane 3, thymus; lane 4, peripheral blood leukocyte; lane 5, bone marrow (BM); and lane 6, fetal liver. The mobility of 285 and 185 rRNA was indicated. (B) Patterns of *Tef* expression in murine myeloid and lymphoid progenitors in different stages of development. cDNA was synthesized from total RNA extracted from 5000 cells of each hematopoietic progenitor subset that had been sorted from bone marrows by FACS (lanes 1-7) as well as unpurified bone marrow mononuclear cells (lane 8). The cDNA was subjected to PCR with primers specific for the murine *Tef* (top panel) and *Hprt* (bottom panel) genes. The PCR product of amplification of *Tef* was subjected to nested PCR (middle panel). HSC indicates hematopoietic stem cells; CMP, common myeloid progenitor; GMP, granulocyte-monocyte progenitor; MEP, megakaryocyte-erythrocyte progenitor; and CLP, common lymphoid progenitor.

and were subjected to reverse transcriptase–PCR (RT-PCR) for *Tef* (Figure 2B).[22] Although *Tef* was detectable in unpurified bone marrow mononuclear cells, the RT-PCR product was virtually undetectable in each subset of progenitors (Figure 2B top panel). Upon performing nested PCR using each PCR product as a template, *Tef* was detected in each subset (Figure 2B middle panel). These results suggested that *Tef* is expressed in hematolymphoid progenitors but its expression is low or restricted to a small fraction of each subset of progenitors.

Establishment of FL5.12 cells conditionally expressing TEF

To analyze the function of TEF in hematopoietic cells, we established FL5.12 cells that inducibly expressed TEF by the addition of Zn using an expression vector (pMT-CB6$^+$) under the control of a metallothionein promoter. Immunoblot analysis using the anti-HLF(C) antibody that effectively recognizes HLF, DBP, and TEF proteins[34] revealed the induction of TEF protein in cells transfected with pMT-TEF when cultured in medium containing 100 μM Zn (Figure 3A lane 4). No endogenous or leaky expression of TEF protein was detected (Figure 3A lanes 1-3). Time course analysis revealed that protein expression of TEF was detectable within 4 hours after the addition of Zn (Figure 3B lane 2) and that it reached a plateau after 16 hours (Figure 3B lanes 4-5). The expression level of TEF was related to the concentration of Zn. Upon the addition of 75 μM Zn, the TEF expression level was approximately 20% of that induced by 100 μM Zn (Figure 3C lanes 4-5), whereas no significant induction was obtained by the addition of less than 50 μM Zn (Figure 3C lanes 2-3). We also established FL5.12 cells that conditionally expressed TEF/BX (Figure 3A lanes 5-6), which is a mutant form of TEF (see "Constructions of eukaryotic expression vectors"), or E2A-HLF (Figure 3A lanes 7 and 8). EMSA using the HLF-CS probe that contains the consensus binding sequence of the PAR proteins[17] detected specific protein-DNA complexes in nuclear extracts from cells expressing either TEF (Figure 3D lanes 3-4) or E2A-HLF (Figure 3D lanes 7-8) but not in nuclear extracts from cells expressing TEF/BX (Figure 3D lanes 5-6). The lack of DNA-binding ability of TEF/BX was not due to aberrant subcellular localization because immunofluorescence studies showed that TEF/BX was localized in the nucleus (data not shown).

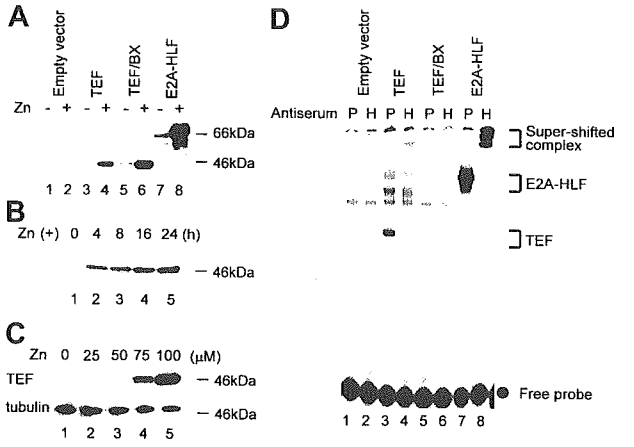

Figure 3. Establishment of FL5.12 cells conditionally expressing TEF, TEF/BX, or E2A-HLF. (A) Immunoblot analysis of FL5.12 cells using HLF(C) antiserum. Representative pools of FL5.12 cells transfected with the empty vector (lanes 1-2), pMT-TEF (lanes 3-4), pMT-TEF/BX (lanes 5-6), or pMT–E2A-HLF (lanes 7-8) were cultured in the presence (even lanes) or absence (odd lanes) of 100 μM $ZnSO_4$ for 16 hours. (B) Time course analysis of TEF expression in pMT-TEF–transfected FL5.12 cells. FL5.12 cells transfected with pMT-TEF were cultured in IL-3–containing medium in the presence of 100 μM Zn for the indicated periods of time and subjected to immunoblot analysis using the HLF(C) antiserum. (C) TEF protein expression in pMT-TEF–transfected FL5.12 cells cultured in the presence of different concentrations of Zn. FL5.12 cells transfected with pMT-TEF were cultured in the presence of Zn at the indicated concentrations for 16 hours and subjected to immunoblot analysis using the HLF(C) antiserum. The expression of tubulin was also analyzed as control. (D) Antibody-perturbed electrophoretic mobility shift analysis (EMSA) with the HLF-CS probe. FL5.12 cells transfected with the empty vector (lanes 1-2), pMT-TEF (lanes 3-4), pMT-TEF/BX (lanes 5-6), or pMT–E2A-HLF (lanes 7-8) were cultured with 100μM of Zn for 16 hours. Nuclear extracts from these cells were incubated with either preimmune (P; odd lanes) or anti-HLF(C) (H; even lanes) antiserum. Brackets show the mobility of DNA-protein complexes containing the indicated proteins and the ● indicates unbound, labeled oligonucleotide probes.

TEF but not E2A-HLF induced G_0/G_1 arrest

When TEF expression was induced by the addition of Zn in proliferating pMT-TEF–transfected FL5.12 cells cultured in IL-3–containing medium, cell growth was gradually disturbed and finally arrested within 36 hours (Figure 4A). In the dye exclusion assay, the viability of TEF-transfected cells was over 90% at 60 hours after the addition of Zn (data not shown). Growth arrest was observed when the Zn concentration was higher than 75 μM (Figure 4B). Cells transfected with pMT-TEF/BX or the empty vector proliferated exponentially in culture medium containing 100 μM Zn (Figure 4A), indicating that the growth inhibition depends on the sequence-specific DNA-binding activity of TEF and not on the cytotoxic effects of Zn. Cells transfected with pMT–E2A-HLF grew more slowly than cells transfected with the empty vector but did not undergo growth arrest (Figure 4A). Growth arrest observed in pMT-TEF–transfected FL5.12 cells was reversible after the withdrawal of Zn (Figure 4C). Cells preincubated in IL-3–containing medium in the presence of 100 μM Zn for 12 hours were washed with medium and subsequently cultured in IL-3–containing medium either in the presence or absence of 100 μM Zn. The expression of TEF was gradually decreased and became undetectable 72 hours after withdrawal of Zn (Figure 4D lanes 3, 5, 7), whereas TEF levels were maintained in the cells that were continued in culture in the presence of Zn (Figure 4D lanes 2, 4, 6). Interestingly, the growth arrest of cells cultured in the absence of Zn was reversed and cells began cycling approximately 72 hours after withdrawal of Zn, whereas the growth arrest and cell viability were maintained in the cells cultured in the presence of Zn (Figure 4C). Moreover, the growth of cells rescued by the withdrawal of Zn could be arrested again upon the subsequent readdition of Zn (Figure 4C).

To determine the cause of growth arrest, cell cycle analysis was performed using flow cytometry (Table 1). Upon the addition of Zn, TEF-expressing cells in the G_0/G_1 phase gradually accumulated and nearly 80% of the cells were in the resting phase after 48 hours. On the other hand, it was unlikely that cell death contributed to this growth arrest because the population in the sub-G_0/G_1 phase always comprised less than 10% of TEF-expressing cells (data not shown). In addition, the G_0/G_1-arrested pMT-TEF–transfected FL5.12 cells were capable of re-entering the cell cycle when Zn was withdrawn from the culture medium (Figure 4E). By contrast, in cells transfected with the empty vector, regardless of the presence or absence of Zn, more than 50% of the cells were in the S phase whereas nearly 40% of the cells were in the G_0/G_1 phase. Consistent with the slow growth rate, the number of E2A-HLF–expressing cells in the S phase slightly decreased after the addition of Zn.

TEF and E2A-HLF promoted cell survival

Next, we analyzed cell viability in the absence of IL-3 (Figure 4F). Cells were precultured in the presence or absence of Zn in IL-3–containing medium for 16 hours, washed with IL-3–free medium twice, and cultured in IL-3–free medium with or without Zn. Cells expressing E2A-HLF survived more than 72 hours in IL-3–free medium, as previously reported.[18,19] TEF also promoted cell survival in IL-3–free medium for 48 hours, but the number of viable cells gradually decreased after 72 hours even though TEF expression was maintained (data not shown). Cells expressing TEF/BX rapidly underwent apoptosis in a manner similar to that of the control cells transfected with the empty vector. These data indicated that TEF protects IL-3–dependent FL5.12 cells from apoptosis in the absence of the cytokine and that this activity depends on its DNA-binding activity.

TEF inactivated IL-3 signaling pathways

To clarify the mechanism of G_0/G_1 arrest induced by TEF, we analyzed the tyrosine phosphorylation of cellular proteins. TEF-transfected cells were preincubated in IL-3–containing medium with Zn for 18 hours, then incubated in IL-3–deficient medium with Zn for 12 hours, and then restimulated by IL-3. As previously reported by others,[43-45] rapid tyrosine phosphorylation of a wide variety of proteins was observed in cells transfected with the empty vector (Figure 5A lanes 1-4) but not in cells expressing TEF (Figure 5A lanes 5-8), suggesting that TEF inactivated signals from the IL-3 receptor. To verify the observation made in Figure 5A more precisely, we analyzed the STAT5 pathway, MAPK pathway, and phosphatidylinositol 3-kinase (PI3K) pathway by monitoring the phosphorylation status of not only STAT5[46] and p44/42 MAPK[47] but also p70S6K[48] and Akt,[49] which are downstream proteins in the PI3K pathway[47] (Figure 5B). Each FL5.12 transfectant was cultured in IL-3–free medium in the presence or absence of Zn for 12 hours following 18 hours' preincubation in IL-3–containing medium with or without Zn, respectively; subsequently exposed to IL-3 for 5 minutes; and processed for immunoblot analysis. In the absence of Zn, IL-3 stimulation of cells transfected with pMT-TEF (Figure 5B lanes 3-4) as well as cells transfected with pMT-TEF/BX (Figure 5B lanes 5-6), pMT–E2A-HLF (Figure 5B lanes 7-8), or the empty vector (Figure 5B lanes 1-2) rapidly induced the phosphorylation of STAT5. In the presence of Zn, phosphorylation of STAT5 was completely abrogated in cells

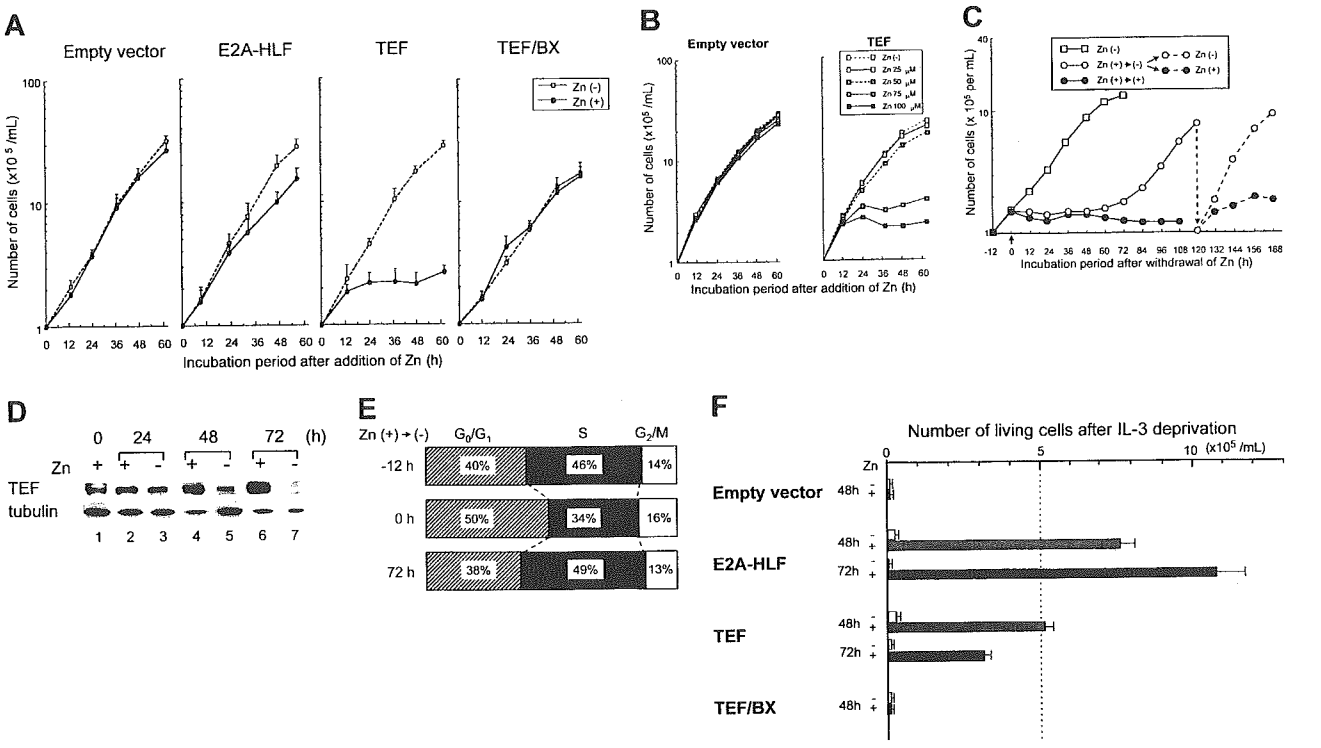

Figure 4. Growth arrest and cell survival of FL5.12 cells transfected with the TEF expression vector. (A) Growth curves of FL5.12 cells transfected with the empty vector, pMT-TEF, pMT-TEF/BX, or pMT–E2A-HLF. Cells were adjusted to 1×10^5 cells per mL and cultured in IL-3–containing medium in the presence (●) or absence (○) of 100 μM Zn. Representative data of multiple experiments using 3 independent pools are shown. Bars indicate standard error. (B) Growth of FL5.12 cells transfected with the empty vector or pMT-TEF in IL-3–containing medium in the presence of 0, 25, 50, 75, or 100 μM of Zn. (C) Growth curves of pMT-TEF–transfected FL5.12 cells after withdrawal of Zn. □ indicates the growth of cells cultured in IL-3–containing medium in the absence of Zn. Cells were preincubated in the presence of 100 μM Zn for 12 hours, washed with medium, adjusted to 1.5×10^5 cells per mL, and then cultured in IL-3–containing medium either in the presence (●) or absence (○) of 100 μM Zn. One hundred twenty hours after withdrawal of Zn, cells cultured in the absence of Zn were adjusted to 1×10^5 cells per mL and cultured in the presence (●- - -●) or absence (○- - -○) of 100 μM Zn. The means of triplicate samples are indicated. (D) Time course analysis of TEF expression in pMT-TEF–transfected FL5.12 cells after withdrawal of Zn. Cells were preincubated in the presence of 100 μM Zn for 12 hours, washed with medium (lane 1), then cultured in IL-3–containing medium in the presence (lanes 2, 4, and 6) or absence (lanes 3, 5, and 7) of 100 μM Zn for the indicated periods of time and subjected to immunoblot analysis using the HLF(C) antiserum. The expression of tubulin was also analyzed as control. (E) Cell cycle analysis of pMT-TEF–transfected FL5.12 cells. Cells cultured in IL-3–containing medium (top; − 12 hours) were preincubated with 100 μM of Zn for 12 hours (middle; 0 hour), washed with medium, and subsequently cultured in IL-3–containing medium in the absence of Zn for 72 hours (bottom; 72 hours). ▨ indicates G_0/G_1; ■, S; and □, G_2/M. (F) Number of viable cells after IL-3 deprivation of FL5.12 cells. FL5.12 cells transfected with the empty vector, pMT-TEF, pMT-TEF/BX, or pMT–E2A-HLF were precultured in IL-3–containing medium in the presence or absence of 100 μM of Zn for 16 hours. Cells were then washed with IL-3–free medium, adjusted to 5×10^5 cells per mL, and cultured without IL-3 either in the presence (▨ and ■) or absence (□) of Zn, respectively. Upon deprivation of IL-3 for 48 or 72 hours, the numbers of viable cells as determined by trypan-blue dye exclusion are indicated. The mean data of 3 independent experiments are shown. Bars indicate standard error.

transfected with the TEF expression vector (Figure 5B lanes 11-12), whereas it was rapidly induced in the other transfectants (Figure 5B lanes 9-10 and 13-16). The same results were observed with regard to the phosphorylation of p44/42 MAPK, p70S6K, and Akt. These results indicated that TEF, acting through its DNA-binding activity, blocked IL-3–signaling pathways whereas E2A-HLF did not. This was supported by the results of EMSA (Figure 5C), which demonstrated rapid induction of protein–DNA complexes containing STAT5 following restoration of IL-3[42] in nuclear extracts from cells transfected with the empty vector (Figure 5C lanes 1-6) but not in cells transfected with pMT-TEF (Figure 5C lanes 7-10).

TEF induces down-regulation of the IL-3 receptor β chains

The inactivation of IL-3 signaling observed in Figure 5 could be explained by down-regulation of the IL-3 receptor by TEF. In mice, the high-affinity IL-3 receptor is a heterodimer of the IL-3–specific α chain and either of the β_{IL3} chain or the β_C chain, the latter of which is shared with the IL-5 and granulocyte-macrophage

Table 1. Cell-cycle analysis of FL5.12 cells in the presence of IL-3

	Empty vector, %			TEF, %			E2A-HLF, %		
Zn⁺, h*	G_0/G_1	S	G_2/M	G_0/G_1	S	G_2/M	G_0/G_1	S	G_2/M
0	37	56	7	32	54	14	30	63	7
8	ND	ND	ND	39	43	17	ND	ND	ND
16	ND	ND	ND	54	27	18	ND	ND	ND
24	41	52	7	61	19	20	47	40	13
48	39	53	8	79	9	12	35	50	14

Data of representative pools of each transfectant are indicated.
ND indicates not determined.
*Hours of incubation with Zn.

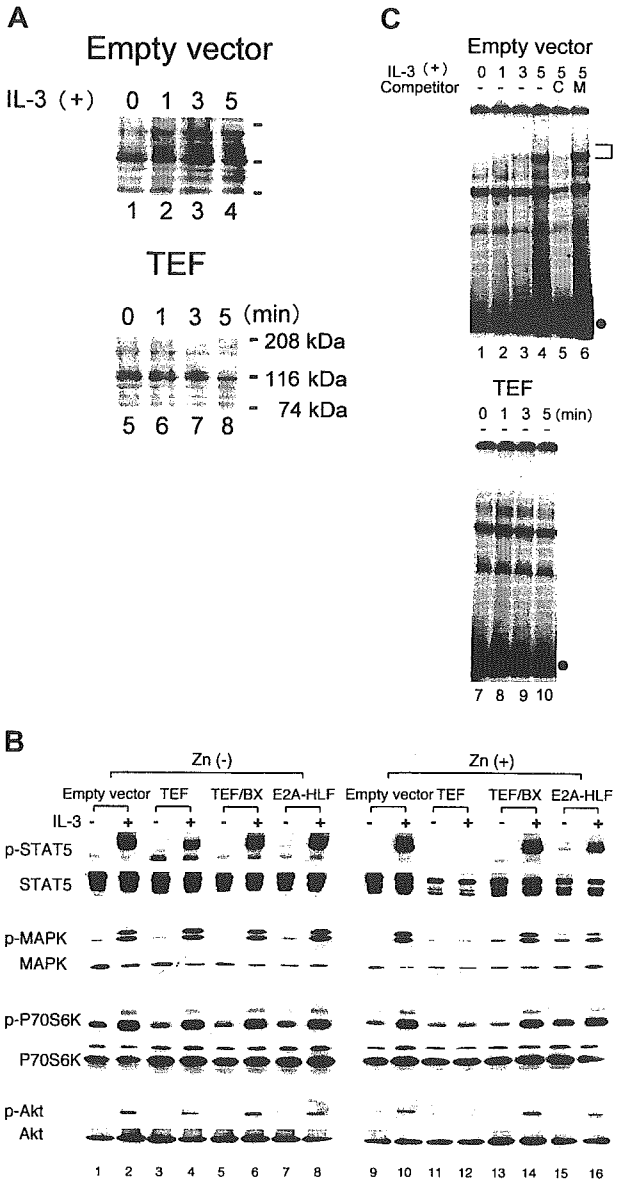

Figure 5. Phosphorylation of cellular proteins by IL-3 restoration. FL5.12 cells transfected with the empty vector, pMT-TEF, pMT-TEF/BX, or pMT–E2A-HLF were cultured in IL-3–containing medium in the presence or absence of Zn for 16 hours, and then the cells were transferred to IL-3–deficient medium in the presence or absence of Zn for 12 hours. Thereafter, cells were restimulated with IL-3 for the indicated periods of time. (A) Immunoblot analysis of FL5.12 cells that had been transfected with the empty vector (lanes 1-4) or pMT-TEF (lanes 5-8) and then cultured in IL-3–containing medium in the presence of Zn using an antiphosphotyrosine monoclonal antibody. (B) Immunoblot analysis for the phosphorylated (p) and nonphosphorylated forms of STAT5, p44/42 MAPK, p70S6K, and Akt in transfectants that had been restored with IL-3 for 5 minutes in the absence (lanes 1-8) or the presence (lanes 9-16) of Zn. The blots were probed with antiphospho-STAT5, antiphospho-p44/42 MAPK, antiphospho-p70 S6K, and antiphospho-Akt as well as anti-STAT5, anti-p44/42 MAPK, anti-p70S6K, and anti-Akt antibodies. (C) Activation of STAT5 DNA-binding by IL-3 restoration. EMSA was performed using nuclear lysates from FL5.12 cells that had been transfected with either the empty vector (lanes 1-6) or pMT-TEF (lanes 7-10) with a β-casein sequence as a probe. In the competition inhibition, an approximately 100-fold molar excess of the unlabeled β-casein sequence oligonucleotide (C; lane 5) or β-casein sequence oligonucleotide with mismatches (M; lane 6) was added in the reaction mixture. A bracket indicates the mobility of specific DNA-protein complexes and ● indicates unbound, labeled oligonucleotide probes.

colony-stimulating factor (GM-CSF) receptors.[50] Northern blot analysis was performed using an α-chain cDNA probe and a β_{IL3} chain cDNA probe; the latter recognizes both the β_{IL3} and β_C transcripts because of their extremely high levels of sequence identity (Figure 6A).[51] Upon the addition of Zn to TEF-transfected cells, the mRNA level of the β chains rapidly decreased and was almost undetectable within 16 hours. In contrast, the addition of Zn to cells transfected with either the empty vector or pMT-TEF did not change the expression level of α-chain mRNA.

Next, we analyzed the cell surface expression of the β_{IL3}, β_C, and α chains of the IL-3 receptor by flow cytometry using specific antibodies for each chain (Figure 6B). Consistent with the results of Northern blot analysis, within 24 hours after the addition of Zn, nearly complete down-regulation of the expression of both the β_{IL3} and β_C chains was observed in cells transfected with pMT-TEF but not in cells transfected with the empty vector, pMT–E2A-HLF, or pMT-TEF/BX. These data indicated that TEF down-regulates expression of the β chains in a DNA-binding–dependent fashion. Moreover, we found up-regulation of the expression of the α chain in TEF-expressing cells but not in cells transfected with the empty vector, pMT-TEF/BX, or pMT-E2A-HLF. Since Northern blot

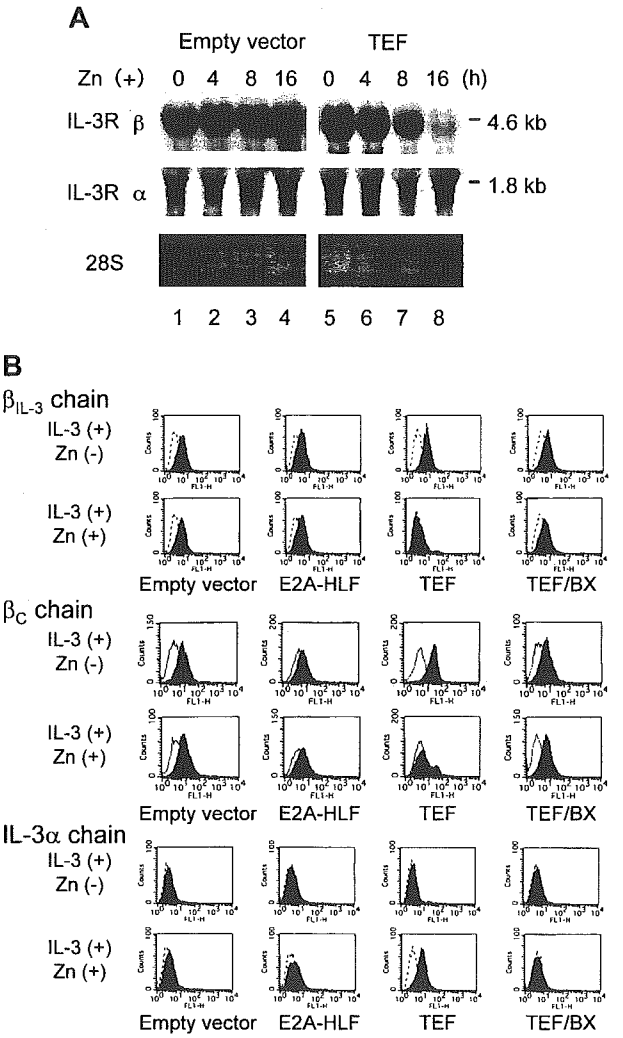

Figure 6. Northern blot analysis and flow cytometric analysis of FL5.12 cells. (A) Northern blot analysis for the IL-3 receptor. Total RNA was extracted from FL5.12 cells that had been transfected with the empty vector (lanes 1-4) or pMT-TEF (lanes 5-8) and cultured in the presence of IL-3 with Zn for the indicated periods of time. The blot was hybridized with mouse cDNA probes specific for IL-3 receptor β chains and α chain. The 28S rRNA visualized with ethidium bromide staining is shown in the bottom panel. (B) Flow cytometric analysis for surface expression of the IL-3 receptor. FL5.12 cells transfected with the empty vector, pMT–E2A-HLF, pMT-TEF, or pMT-TEF/BX were cultured in IL-3–containing medium in the presence or absence of Zn for 24 hours. Cells were analyzed with the specific antibodies for mouse β_{IL3}, β_C, or α chains. Dotted or solid lines indicate the histograms of control staining, and filled curves indicate those of specific antibodies.

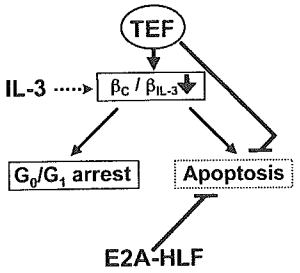

Figure 7. Hypothetical roles of TEF and E2A-HLF. TEF down-regulates the expression of the common β (β_C) chain and inactivates IL-3 signaling pathways, which are critical for both cell proliferation and cell survival. In addition, TEF promotes cell survival in the absence of survival signalings downstream of IL-3. Consequently, cells in the G_0/G_1 phase accumulated without undergoing apoptosis. In contrast, E2A-HLF blocks apoptosis without regulating the expression of cytokine receptors.

analysis revealed that the level of mRNA expression of the α chain did not change (Figure 6A), up-regulation of the cell surface α-chain expression by TEF was due to posttranscriptional mechanism(s), probably inhibition of internalization caused by down-regulation of the expression of β chains.[52] These observations indicated that TEF disrupts formation of the IL-3 receptor by down-regulating the cell surface expression of the β chains, thus rendering FL5.12 cells insensitive to IL-3.

Discussion

In this study, using a Zn-inducible system, TEF protein expression was induced in pMT-TEF–transfected FL5.12 cells within 4 hours after the addition of Zn (Figure 3B). The mRNA expression levels of the β subunits of the IL-3 receptor were reduced and became barely detectable within 16 hours (Figure 6A), and surface expression of the β chains was almost completely down-regulated within 24 hours (Figure 6B). Subsequently, the IL-3 signaling pathways were lost (Figure 5) and cells underwent cell cycle arrest in G_0/G_1 phase within 36 hours (Figure 4A; Table 1). However, the cells did not undergo apoptosis (Figure 4A) because TEF protected FL5.12 cells from apoptosis induced by IL-3 deprivation (Figure 4F). Thus, TEF induced FL5.12 cells to remain in a resting state, either in the presence or absence of IL-3 (Figure 7). These unique functions of TEF depended on its DNA-binding potential because a TEF mutant with amino acid substitutions in its basic region (TEF-BX) completely lost these activities (Figures 4-6). However, there is no potential binding site for TEF in the promoter regions of the 2 β-chain genes in the mouse[51,53] and TEF is known as a transcriptional activator.[29,37] Thus, TEF likely down-regulates transcription of the β-chain genes indirectly.

The β_C chain is common to the receptors of a series of major cytokines including IL-5 and GM-CSF as well as IL-3 and is expressed by the majority of hematopoietic progenitors (H.I. and A.K., unpublished observation, May 2004; Militi et al[54]), which expand in response to multiple growth factors during normal hematopoiesis. Therefore, it is reasonable that the *Tef* expression level in each hematolymphoid progenitor was low (Figure 2B). TEF expression may be restricted to a small fraction of progenitors that are in the resting phase and do not express the β_C chain. TEF might play an important role in preventing the exhaustion of hematopoietic progenitors by rendering a portion of the progenitors to be insensitive to growth factors. Establishment of Tef-deficient mice and extensive analysis of their hematopoiesis would elucidate the biologic significance of this unique transcription factor that regulates both cell survival and expression of cytokine receptors in hematopoietic progenitors.

This study also provides insights into functional differences between oncogenic chimeras and their normal counterparts. Similar to TEF, the E2A-HLF chimera inhibited apoptosis caused by IL-3 deprivation (Figure 4F; Inaba et al,[18] Inukai et al,[19] Altura et al[20]). However, unlike TEF, E2A-HLF did not down-regulate the expression of β subunits of the IL-3 receptor. As a result, cells expressing E2A-HLF proliferated in the presence of IL-3 (Figure 4A) and survived in the absence of IL-3 (Figure 4F). These findings suggest that the chimeric transcription factor retains the ability to drive leukemic transformation with maximum efficiency by disrupting multiple transcriptional networks. Since TEF and HLF share a high degree of sequence identity in their bZIP domains, the difference in the ability to regulate the levels of growth factor receptors between TEF and E2A-HLF is most likely caused by differences in their *trans*-activation domains (Figure 1). Alternatively, subtle changes in their DNA-binding specificity might contribute to the loss of activity of E2A-HLF to regulate cytokine receptors. The DNA-binding specificity of the PAR bZIP transcription factors is reported to be influenced by the sequences flanking the basic region, such as the basic region extension (BRE), fork region, and PAR domains.[36] Because the BRE and PAR domains of HLF are not included in the E2A-HLF chimera (Figure 1), the DNA-binding potential of E2A-HLF to suboptimal sites is substantially impaired.[34]

The antiapoptotic potential of TEF that depends on its DNA-binding activity supports a model that the consensus binding sequence recognized by the PAR factors as well as E2A-HLF, E4BP4, and CES-2 could serve as a regulatory switch for programmed cell death.[18-20,23,24] However, the detailed downstream pathways in mammalian systems have not yet been elucidated. In *C elegans*, CES-2 appears to down-regulate CES-1 expression.[5,6] Although we previously identified the *SLUG* gene, a mammalian homologue of CES-1, as one of the downstream responders of E2A-HLF in human leukemia cells with t(17;19) translocation,[23] neither TEF nor E2A-HLF was able to induce its expression in FL5.12 cells (data not shown). Thus, there must be other critical downstream pathway(s) for the antiapoptotic potential of TEF and E2A-HLF. Identification of downstream pathway(s) of TEF for its antiapoptotic potential and β_{IL3} and β_C chain gene regulation will be critical for clarifying transcriptional regulation driving normal hematopoiesis as well as leukemogenesis by E2A-HLF.

Acknowledgments

We are indebted to Dr F. Rauscher III for providing the pMT-CB6+ Zn inducible vector. This research was supported by grants-in-aid from the Ministry of Education, Science and Culture of Japan.

References

1. Horvitz HR, Shahan S, Hengarter MO. The genetics of programmed cell death in the nematode *Caenorhabditis elegans*. Cold Spring Harb Symp Quant Biol. 1994;59:377-385.
2. Ellis RE, Horvitz HR. Two *C. elegans* genes control the programmed deaths of specific cells in the pharynx. Development. 1991;112:591-603.
3. Metzstein M, Hengartner M, Tsung N, Ellis R, Horvitz HR. Transcriptional regulator of programmed cell death encoded by *Caenorhabditis elegans* gene *ces-2*. Nature. 1996;382:545-547.
4. Metzstein M, Horvitz HR. The *C. elegans* cell death specification gene ces-1 encodes a Snail family Zn finger protein. Mol Cell. 1999;4:309-319.

5. Conradt B, Horvitz HR. The *C. elegans* protein EGL-1 is required for programmed cell death and interacts with the Bcl-2-like protein CED-9. Cell. 1998;93:519-529.
6. Jacobson MD. Programmed cell death: a missing link is found. Trends In Cell Biol. 1997;7:467-469.
7. Thellmann M, Hatzold J, Conradt B. The Snail-like CES-1 protein of *C. elegans* can block the expression of the *BH3-only* cell-death activator gene *egl-1* by antagonizing the function of bHLH proteins. Development. 2003;130:4057-4071.
8. Hunger S, Ohyashiki K, Toyama K, Cleary M. Hlf, a novel hepatic bZIP protein, shows altered DNA-binding properties following fusion to E2A in t(17; 19) acute lymphoblastic leukemia. Genes Dev. 1992;6:1608-1620.
9. Hunger S. Chromosomal translocation involving the *E2A* gene in acute lymphoblastic leukemia: clinical features and molecular pathogenesis. Blood. 1996;87:1211-1224.
10. Inaba T, Roberts M, Shapiro L, et al. Fusion of the leucine zipper gene *HLF* to the *E2A* gene in human acute B-lineage leukemia. Science. 1992; 257:531-534.
11. Yoshihara T, Inaba T, Shapiro L, Kato J, Look AT. E2A-HLF-mediated cell transformation requires both the transactivation domains of E2A and the leucine zipper dimerization domain of HLF. Mol Cell Biol. 1995;15:3247-3255.
12. Inukai T, Inaba T, Yoshihara T, Look AT. Cell transformation mediated by homodimeric E2A-HLF transcription factors. Mol Cell Biol. 1997;17:1417-1424.
13. Matsunaga T, Inaba T, Matsui H, et al. Regulation of annexin II by cytokine-initiated signaling pathways and E2A-HLF oncoprotein. Blood. 2004; 103:3185-3191.
14. Kurosawa H, Goi K, Inukai T, et al. Two candidate downstream target genes for E2A-HLF. Blood. 1999;93:321-332.
15. Dang J, Inukai T, Kurosawa H, et al. The-E2A-HLF oncoprotein activates groucho-related genes and suppresses runx1. Mol Cell Biol. 2001;21: 5935-5945.
16. Honda H, Inaba T, Suzuki T, et al. Expression of E2A-HLF chimeric protein induced T-cell apoptosis, B-cell maturation arrest, and development of acute lymphoblastic leukemia. Blood. 1999;93: 2780-2790.
17. Smith KS, Rhee JW, Naumovski L, Cleary ML. Disrupted differentiation and oncogenic transformation of lymphoid progenitors in E2A-HLF transgenic mice. Mol Cell Biol. 1999;19:4443-4451.
18. Inaba T, Inukai T, Yoshihara T, et al. Reversal of apoptosis by the leukaemia-associated E2A-HLF chimeric transcriptional factor. Nature. 1996;382: 541-544.
19. Inukai T, Inaba T, Ikushima S, Look AT. Antiapoptotic role of the AD1 and AD2 transactivation domains of E2A in pro-B lymphocytes deprived of growth factor. Mol Cell Biol. 1998;18:6035-6043.
20. Altura R, Inukai T, Ashmun R, et al. The chimeric E2A-HLF transcription factor abrogates p53-induced apoptosis in myeloid leukemia cells. Blood. 1998;92:1397-1405.
21. Inukai T, Inoue A, Kurosawa H, et al. *SLUG*, a *ces-1*-related Zn-finger transcription factor gene with antiapoptotic activity, is a downstream target of the E2A-HLF oncoprotein. Mol Cell. 1999;4: 343-352.
22. Inoue A, Seidel MG, Wu W, et al. Slug, a highly conserved zinc finger transcriptional repressor, protects hematopoietic progenitor cells from radiation-induced apoptosis in vivo. Cancer Cell. 2002;2:279-288.
23. Ikushima S, Inukai T, Inaba T, et al. Pivotal role of the NFIL3/E4BP4 transcription factor in interleukin 3-mediated survival of pro-B lymphocytes. Proc Natl Acad Sci U S A. 1997;94:2609-2614.
24. Kuribara R, Kinoshita T, Miyajima A, et al. Two distinct interleukin-3-mediated signal pathways, Ras-NFIL3 (E4BP4) and Bcl-x_L, regulate the survival of murine pro-B lymphocytes. Mol Cell Biol. 1999;19:2754-2767.
25. Drolet D, Scully K, Simmons D, et al. TEF, a transcription factor expressed specifically in the anterior pituitary during embryogenesis, defines a new class of leucine zipper proteins. Genes Dev. 1991;5:1739-1753.
26. Mueller CR, Maire P, Schibler U. DBP, a liver-enriched transcriptional activator, is expressed late in ontogeny and its tissue specificity is determined posttranscriptionally. Cell. 1990;61:279-291.
27. Wuarin J, Schibler U. Expression of the liver-enriched transcriptional activator protein DBP follows a stringent circadian rhythm. Cell. 1990;63: 1257-1266.
28. Falvey E, Fleury-Olela F, Schibler U. The rat hepatic leukemia factor (HLF) gene encodes two transcriptional activators with distinct circadian rhythms, tissue distributions and target preferences. EMBO J. 1995;14:4307-4313.
29. Fonjallaz P, Ossipow V, Wanner G, Schibler U. The two PAR leucine zipper proteins, TEF and DBP, display similar circadian and tissue-specific expression, but have different target promoter preferences. EMBO J. 1996;15:351-362.
30. Lopez-Molina L, Conquet F, Dubois-Dauphin M, Schibler U. The DBP gene is expressed according to a circadian rhythm in the suprachiasmatic nucleus and influences circadian behavior. EMBO J. 1997;16:6762-6771.
31. Balsalobre A, Damiola F, Schibler U. A serum shock induces circadian gene expression in mammalian tissue culture cells. Cell. 1998;93: 929-937.
32. Yamaguchi S, Mitsui S, Yan L, et al. Role of DBP in the circadian oscillatory mechanism. Mol Cell Biol. 2000;20:4773-4781.
33. Mitsui S, Yamaguchi S, Matsuo T, Ishida Y, Okamura H. Antagonistic role of E4BP4 and PAR proteins in the circadian oscillatory mechanism. Genes Dev. 2001;15:995-1006.
34. Hunger S, Brown R, Cleary M. DNA-binding and transcriptional regulatory properties of hepatic leukemia factor (HLF) and the t(17;19) acute lymphoblastic leukemia chimera E2A-HLF. Mol Cell Biol. 1994;14:5986-5996.
35. Inaba T, Shapiro L, Funabiki T, et al. DNA-binding specificity and trans-activating potential of the leukemia-associated E2A-hepatic leukemia factor fusion protein. Mol Cell Biol. 1994;14:3403-3413.
36. Haas N, Cantwell C, Johnson P, Burch J. DNA-binding specificity of the PAR basic leucine zipper protein VBP partially overlaps those of the C/EBP and CREB/ATF families and is influenced by domains that flank the core basic region. Mol Cell Biol. 1995;15:1923-1932.
37. Hunger S, Li S, Fall M, Naumovski L, Cleary M. The proto-oncogene HLF and the related basic leucine zipper protein TEF display highly similar DNA-binding and transcriptional regulatory properties. Blood. 1996;87:4607-4617.
38. Hara T, Miyajima A. Two distinct functional high affinity receptors for mouse interleukin-3 (IL-3). EMBO J. 1992;11:1875-1884.
39. Ogorochi T, Hara T, Wang H, Maruyama K, Miyajima A. Monoclonal antibodies specific for low-affinity interleukin-3 (IL-3) binding protein AIC2A: evidence that AIC2A is a component of a high-affinity IL-3 receptor. Blood. 1992;79:895-903.
40. Khatib Z, Inaba T, Valentine M, Look AT. Chromosomal localization and cDNA cloning of the human DBP and TEF genes. Genomics. 1994;23: 344-351.
41. Akashi K, Traver D, Miyamoto T, Weissman IL. A clonogenic common myeloid progenitor that give rise to all myeloid lineages. Nature. 2000;404: 193-197.
42. Mui A, Wakao H, O'Farrell A, Harada N, Miyajima A. Interleukin-3, granulocyte-macrophage colony stimulating factor and interleukin-5 transduce signals through two STAT5 homologs. EMBO J. 1995; 14:1166-1175.
43. Isfort R, Huhn R, Frackelton A, Ihle J. Stimulation of factor-dependent myeloid cell lines with interleukin 3 induces tyrosine phosphorylation of several cellular substrates. J Biol Chem. 1988;35: 19203-19209.
44. Duronio V, Clark-Lewis I, Federsppiel B, Wieler J, Schrader J. Tyrosine phosphorylation of receptor beta subunits and common substrates in response to interleukin-3 and granulocyte-macrophage colony-stimulating factor. J Biol Chem. 1992;30:21856-21863.
45. Silvennoinen O, Witthuhn B, Quelle F, Cleveland J, Ihle J. Structure of the murine Jak2 protein-tyrosine kinase and its role in interleukin 3 signal transduction. Proc Natl Acad Sci U S A. 1993;90: 8429-8433.
46. Dumon S, Santos SC, Debierre-Grockiego F, et al. IL-3 dependent regulation of Bcl-xL gene expression by STAT5 in a bone marrow derived cell line. Oncogene. 1999;18:4191-4199.
47. Kinoshita T, Miyajima A. Raf/MAPK and rapamycin-sensitive pathway mediate the anti-apoptotic function of p21Ras in IL-3-dependent hematopoietic cells. Oncogene. 1997;15:619-627.
48. Reif K, Burgering B, Cantrell D. Phosphatidylinositol 3-kinase links the interleukin-2 receptor to protein kinase B and p70 S6 kinase. J Biol Chem. 1997;272:14426-14433.
49. Dudek H, Datta SR, Franke TF, et al. Regulation of neuronal survival by the serine-threonine protein kinase Akt. Science. 1997;275:661-665.
50. Miyajima A, Mui AL, Ogorochi T, Sakamaki K. Receptor for granulocyte-macrophage colony-stimulating factor, interleukin-3, and interleukin-5. Blood. 1993;82:1960-1974.
51. Gorman D, Itoh N, Jenkins N, et al. Chromosomal localization and organization of the murine genes encoding the β subunits (AIC2A and AIC2B) of the interleukin 3, granulocyte/macrophage colony-stimulating factor, and interleukin 5 receptors. J Biol Chem. 1992;22:15842-15848.
52. Algate P, Steelman L, Mayo M, Miyajima A, McCubrey J. Regulation of the interleukin-3 (IL-3) receptor by IL-3 in the fetal liver-derived FL5.12 cell line. Blood. 1994;83:2459-2468.
53. van Dijk T, Baltus B, Caldenhoven E, et al. Cloning and characterization of the human interleukin-3 (IL-3)/IL-5/granulocyte-macrophage colony-stimulating factor receptor βc gene: regulation by Ets family members. Blood. 1998;92:3636-3646.
54. Militi S, Riccioni R, Parolini I, et al. Expression of interleukin 3 and granulocyte-macrophage colony-stimulating factor receptor common chain β_C, β_{IT} in normal hematopoiesis: lineage specificity and proliferation-independent induction. Br J Hematol. 2000;111:441-451.

Molecular Biology Reports (2005) 32: 79–85
DOI 10.1007/s11033-004-7656-0

Structure of the human *Bim* gene and its transcriptional regulation in Baf-3, interleukin-3-dependent hematopoietic cells

Hirotaka Matsui[1], Tetsuharu Shinjyo[2] & Toshiya Inaba[1,*]
[1]*Department of Molecular Oncology & Leukemia Program Project, Research Institute for Radiation Biology and Medicine, Hiroshima University, Hiroshima, 734–8553, Japan;* [2]*Second Department of Internal Medicine, University of Ryukyus, Okinawa, 903-0215, Japan; *Author for correspondence (Phone: +81-82-257-5834; Fax: +81-82-256-7103; E-mail: tinaba@hiroshima-u.ac.jp)*

Accepted 6 December 2004

Key words: apoptosis, Bim, cytokine, reporter assay, transcriptional regulation

Abstract

Deprivation of cytokines induces cell cycle arrest and apoptosis in cytokine-dependent hematopoietic progenitors. Previous studies have indicated that in Baf-3, interleukin (IL)-3-dependent cells, apoptosis is caused predominantly by *Bim*, a BH3-only cell death activator that belongs to the Bcl-2 superfamily. Because *Bim* mRNA is induced by IL-3 starvation, we hypothesized that signals originating from the IL-3 receptor might regulate the expression of *Bim* at the level of its transcription. Here, we identified the transcriptional initiation site and three candidate remote enhancer/silencer regions of the *Bim* gene. We show that the region of the gene upstream of the initiation site exhibits strong promoter activity and that there are negative regulatory regions within the first intron. However, none of these transcriptional regulatory elements was IL-3-dependent. In addition, a nuclear run-off assay revealed a similar rate of transcription initiation in the absence or presence of IL-3. Although others have demonstrated the transcriptional regulation of *Bim* by nerve growth factor (NGF) in neuronally differentiated PC12 pheochromocytoma cells, this is unlikely to be the mechanism through which IL-3 downregulates the expression of *Bim* in Baf-3 cells.

Abbreviations: NGF – nerve growth factor; RACE – 5′-rapid amplification of cDNA ends; RPA – ribonuclease protection assay.

Introduction

Pathways through which cytokine receptors transmit signals to support cell survival have been under intensive investigation. Such studies frequently employ murine interleukin (IL)-3-dependent cells, such as Baf-3 or 32D cells (reviewed in reference [1]). Experiments using Baf-3 cells have demonstrated that the IL-3-dependent activation of Ras, especially the Ras/Raf/MAPK or Ras/PI3-K pathways, is essential for long-term cell survival [2, 3]. The pivotal downstream targets of these pathways are likely to be members of the Bcl-2 superfamily, which includes more than 15 factors in mammals, and each of which mediates distinct death triggers (reviewed in reference [4]). We recently demonstrated that Bim [5, 6], a BH3-only cell death activator in the Bcl-2 superfamily, plays a critical role in the regulation of apoptosis in Baf-3 cells in a IL-3-dependent manner. [7, 8]. The importance of Bim in hematopoiesis has also been demonstrated in Bim-deficient mice, which exhibit

hyperplasia of hematopoietic progenitors in the bone marrow and increase in the white blood cell count in the peripheral blood [9].

The function of Bim has been reported to be regulated by at least four different mechanisms. First, the expression of its mRNA is reduced by IL-3 in IL-3-dependent Baf-3 and FL5.12 cells [7, 8] and by nerve growth factor (NGF) in NGF-dependent neuronal cells, including primary cultures of rat sympathetic neurons or neuronally differentiated PC-12 cells [10–12]. Second, Bim protein is regulated by proteasome-dependent degradation in serum-deprived fibroblasts and M-CSF-dependent osteoclasts [13, 14]. The phosphorylation of Bim induced by serum or cytokines enhances the efficiency of its ubiquitination. Third, the subcellular localization of Bim is controlled by IL-3 in FDC-P1 cells or by exposure of 293 cells to ultraviolet light [15, 16]. Finally, phosphorylation of Bim by NGF in neuronally differentiated PC-12 cells has been reported to suppress its proapoptotic activity, but not its subcellular localization [10]. These diverse regulatory mechanisms suggest that the function of Bim can be regulated in different ways in certain situations and that the relative importance of these four mechanisms may differ between cell types [17]. Among these regulatory mechanisms, the control of mRNA expression is likely to be important in hematopoiesis, because we recently found that both Bim mRNA and protein are induced by cytokine-deprivation in early hematopoietic progenitors ($Sca\text{-}1^+c\text{-}Kit^+Lin^-$) isolated from primary murine bone marrow culture [18]. Thus, we decided to test whether downregulation of Bim mRNA by IL-3 in Baf-3 cells is mediated through a transcriptional mechanism similar to that shown recently in neuronally differentiated PC12 cells, whereby Bim mRNA is downregulated by NGF [19].

Materials and methods

Cell lines and cell culture

Baf-3, a murine IL-3-dependent cells were cultured in RPMI-1640 medium containing 10% fetal calf serum (FCS), 20 mM Hepes, 50 μM 2-mercaptoethanol, and 0.5% 10T1/2-conditioned medium as a source of murine IL-3. To deplete IL-3, we washed the cells twice with IL-3-free growth medium. HL60, a human myeloid leukemia cell line was maintained in RPMI-1640 supplemented with 10% FCS.

5′-rapid amplification of cDNA ends (RACE) and ribonuclease protection assay (RPA)

5′-RACE was performed using SMART RACE cDNA amplification kit (Clontech, Palo Alto, CA) according to the manufacturer's instruction. The gene specific reverse primer used in this procedure is 5′-TTGTGGCTCTGTCTGTAGGGAGG TAG-3′ in exon 2 of human *Bim* gene. RPA was performed using a kit (Ambion, Austin, TX) according to the manufacturer's direction. Briefly, total RNA (10 μg each) was hybridized with [^{35}S]UTPαS-labeled RNA probes (probes 1–5). Probe 1 starts its 5 end at 5 base upstream of the initiation site, probe 2 at 1 base upstream, probe 3 at the initiation site, probe 4 at 1 base downstream of the initiation site, and probe 5 at 5 base downstream. After digesting single-stranded RNA by RNaseA, samples were separated on a 5% acrylamide/8 M urea gel and viewed by autoradiography.

DNase I hypersensitivity assay

Nuclei of HL60 cells were isolated by the treatment of hypotonic buffer contained in a DNA extraction kit (Qiagen, Hilden, Germany). After incubation of nuclei with sequential dilution of DNase I (Loche, Mannheim, Germany) for 3 min at room temperature, genomic DNA was extracted and digested with restriction enzymes indicated in the legend of Figure 2. DNA was blotted on nylon membrane and subjected to be hybridized with [^{32}P]-labeled genomic probes in human *Bim* gene and its flanking region.

Transcriptional assay

Baf-3 cells were transiently transfected with reporter plasmids (30 μg) containing candidates of the promoter and enhancer of human *Bim* gene in front of the luciferase gene in the pGL3-basic plasmid (Promega, Madison, WI) along with 5 μg of pRL-tk as an internal control to normalize luciferase activities for transfection efficiency. Six hours later, cells were divided into two dishes and were continued to culture in the presence or

absence of IL-3 for 16 h. Luciferase assays using the Fluroskan Ascent luminometer (Labsystems, Helsinki, Finland) were performed by Dual luciferase assay systems (Promega) according to the manufacturer's instructions. Relative luciferase activity was calculated by dividing luciferase activity of each construct by that of the empty pGL3-basic reporter plasmid.

Nuclear run off assay

Nuclei of Baf-3 cells were isolated using hypotonic buffer (10 mM HEPES pH7.9, 1.5 mM $MgCl_2$, 10 mM KCl) and mRNA were elongated in labeling solution (20 mM Tris pH 8.0, 140 mM KCl, 10 mM $MgCl_2$, 20% v/v glycerol, 14 mM 2-mercaptoethanol, 1 mM ATP, CTP, and GTP, 10 mM phosphocreatine, 100 μg/ml phosphocreatine kinase, 21 μl [^{32}P]-UTP) for 30 min at 30 °C. RNA was then extracted using Isogen RNA extraction kit (Wako Pure Chemicals, Osaka, Japan) and hybridized with dot blot nylon membrane. Each dot contains 20 μg plasmid DNA containing cDNA of mouse Bim, Bcl-x_L or β-actin.

Results and discussion

Isolation of promoter and candidate remote enhancer regions of human Bim *gene*

Comparison of the human genomic sequence of Bim derived from Human Genome Resources on the website of the National Center for Biotechnology Information with that of the human *Bim* mRNA as well as EST clones deposited in the Genbank database revealed that this gene has six exons spanning approximately 40 kb on chromosome band 2q13 (Figure 1a). The *Bim* gene was flanked by two predicted genes (Locus IDs 55289 and 376939), each of which encodes a hypothetical protein, FLJ11042 or ENSANGP00000004103, respectively.

To isolate the *cis*-acting DNA elements of the human *Bim* gene, we first identified its transcriptional initiation site in HL60 human myeloid leukemia cells, which express *Bim* mRNA at high levels (data not shown). We identified a putative transcriptional initiation site 16 bp upstream (5′) of the extreme 5′-most sequence of a known EST clone (accesion no. BX282330) by 5′ RACE analysis (Figure 1b). We confirmed this site by an RNase protection assay (Figure 1c). We prepared five radiolabeled probes with an identical 3′ end, but different 5′ ends in the proximity of the putative transcriptional initiation site (Figure 1c, lanes 1–5). The radiolabeled probes were hybridized to total RNA extracted from HL60 cells. Bands protected by probe 1 (5′ end: five bases upstream of the putative initiation site), by probe 2 (one base upstream) and by probe 3 (at the putative initiation site) were identical in size (arrow, lanes 6–8), while those protected by probe 4 (one base downstream of the putative initiation site) and by probe 5 (five bases downstream) were proportionately shorter in size (open arrowheads, lanes 9 and 10), indicating that the site determined by 5′ RACE analysis is the *bonafide* trancription initiation site in HL60 cells. There are no putative TATA or CAAT box elements in the region upstream of the transcriptional initiation site (Figure 1b).

To confirm the upstream promoter region identified above and to find out candidate enhancer/silencer regions, we searched sites of DNase I hypersensitivity within an approximately 130 kb genomic fragment containing the entire *Bim* gene (Figure 1a). We identified four DNase I hypersensitive regions. Two (TE1 and TE2) were located in the upstream (5′) region of the *Bim* gene (Figures 2a and 2b), a third (Pr) corresponded to the upstream promoter region, as well as the entire sequence of exon 1 and a part of the first intron (Figure 2c), and a fourth (TE3) was located in the downstream (3′) region of the gene (Figure 2d). All hypersensitive regions were confirmed by analyses with at least two different restriction enzymes and probes.

Lack of cytokine-dependent cis-acting DNA elements of Bim *gene*

We then made a series of reporter plasmid constructs by cloning different fragments from the promoter region upstream of the luciferase gene in the pGL3-Basic vector (Figure 3a, 2–9). IL-3-dependent Baf-3 cells were transfected with these reporter plasmids by electroporation. Six hours later, cells were washed with IL-3-free medium and divided into two cultures, which either contained or did not contain IL-3, and the cells were cultured for an additional 16 h. We detected promoter

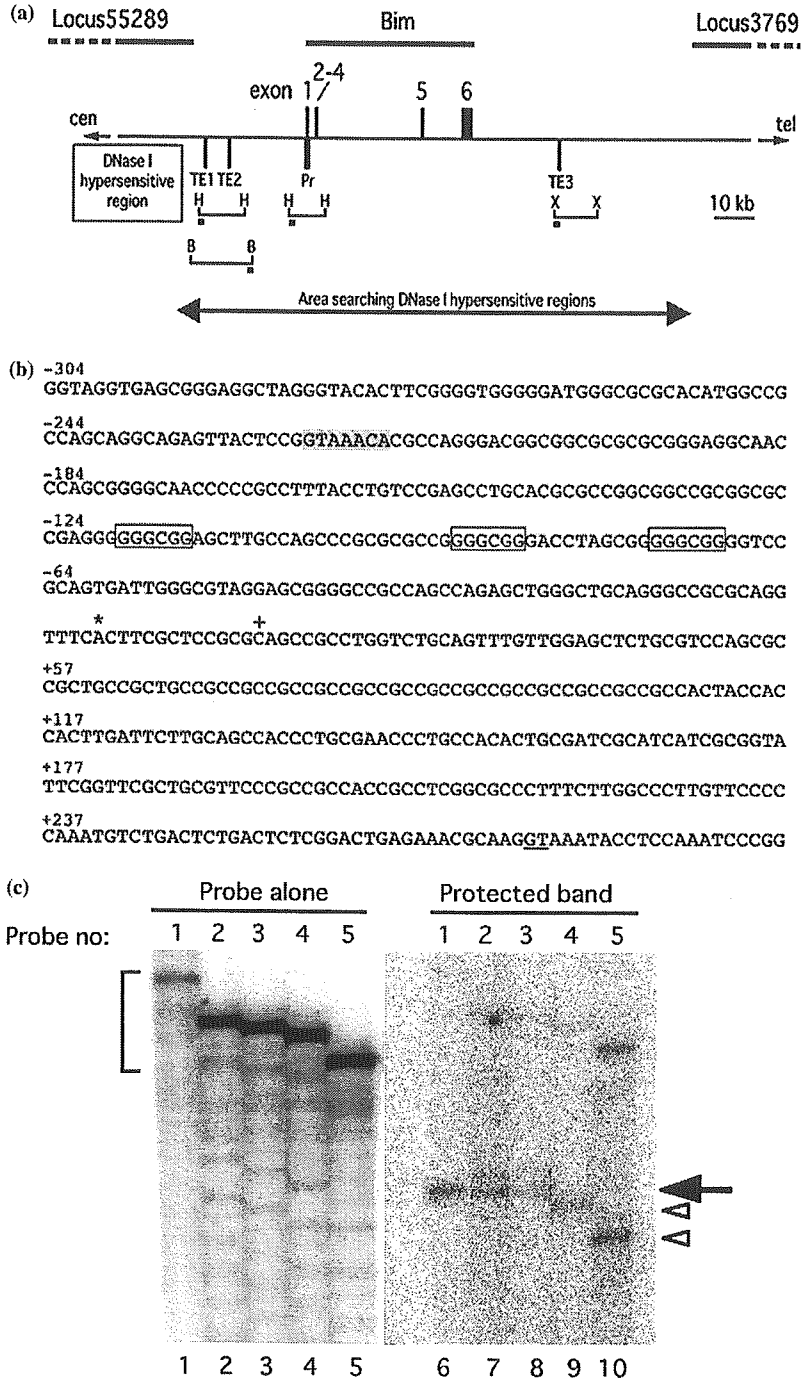

Figure 1. The human *Bim* gene. (a) A genomic map of the human *Bim* gene on chromosome band 2q13. The *Bim* gene contains six exons and is flanked by loci 55289 and 376939. The four DNase I hypersensitive regions (TE1, TE2, Pr, and TE3) identified by the DNase I hypersensitive assay are indicated. The restriction enzyme fragments used in this assay are shown below. Bars indicate the position of the probes used in this assay. B, *Bam*HI; H, *Hind*III; X, *Xba*I. (b) The genomic DNA sequence of the upstream promoter region, exon 1, and a part of the first intron. An asterisk (*) indicates the transcriptional initiation site, and a plus sign (+) indicates the extreme 5' sequence of a known EST clone (accesion no. BX282330). The core consensus binding sites of Sp1 are shown by open boxes, while that of FOXO3a is shaded gray. The splice donor site of the first intron is underlined. (c) Ribonuclease protection assay. [^{32}P]-labeled probes 1–5 (see text) were hybridized to 10 μg total RNA extracted from HL60 cells. After digestion of single-stranded RNA with RNase A, samples (lanes 6–10) and untreated probes (lanes 1–5) were separated on a 5% acrylamide/8 M urea gel and viewed by autoradiography. A bracket shows probes. An arrow and arrowheads indicate protected bands.

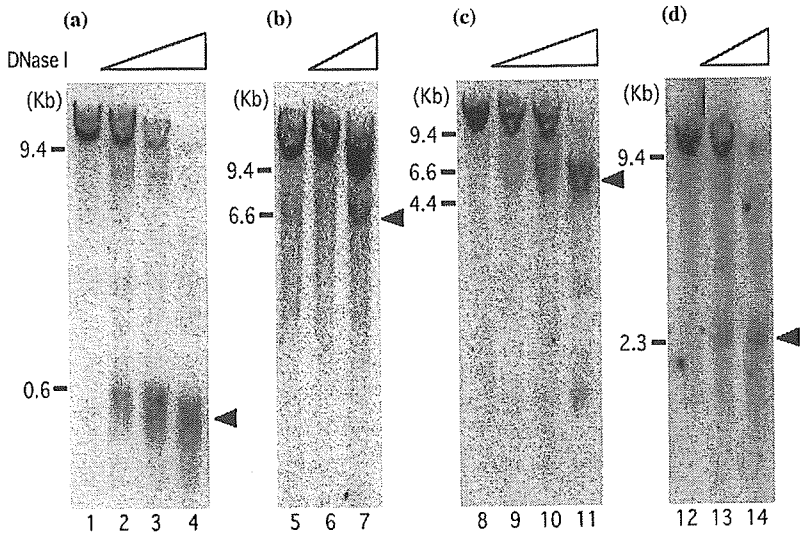

Figure 2. DNase I hypersensitivity assay. Nuclei from HL60 cells were digested with sequential dilutions of DNase I for 3 min at room temperature. Genomic DNA was then extracted and digested with *Hind*III (a) (c), *Bam*HI (b), or *Xba*I (d) restriction enzymes. DNA fragments were blotted onto a nylon membrane and hybridized to the radiolabeled genomic probes indicated in Figure 1a.

activity when the reporter construct contained a 92-bp fragment upstream of the transcription initiation site (#3). Robust luciferase expression was observed following transfection of cells with reporter constructs that contained fragments of the promoter region of increasing size, from 122-bp to 874-bp upstream of the initiation site (#4–#9). These studies suggested that the region of the promoter from −68 to −147 is essential to drive Bim expression, as has been previously reported for the mouse homolog (Figure 3a) [20]. Examination of the sequence revealed that this region is extremely GC-rich (88.8% G+C) and that it contains three core binding sites for the Sp-1 transcription factor (GGGCGG) (Figure 1b). The promoter activity was not significantly different between cultures in the presence or absence of IL-3. To test the possibility that (a) remote enhancer/silencer region(s) function as cytokine-dependent *cis*-acting elements, we cloned genomic DNA fragments containing TE1, TE2, or TE3 and inserted them downstream of the luciferase gene in a reporter construct that also contained a 302 bp fragment upstream of the transcription initiation site (#10–#12). Although TE3 suppressed *trans*-activation by the proximal promoter region, this effect was not cytokine dependent.

Because the first intron of genes frequently contain *cis*-acting elements, we inserted the entire sequence of the first intron between the promoter/exon 1 sequence and the luciferase gene in the reporter plasmid (Figure 3b, #14). We observed a marked reduction in the activity of the promoter, indicating that silencer region(s) are located within the first exon. Indeed, three constructs (#17, #18, and #20) suppressed the *trans*-activation potential of the promoter region of *Bim*. However, none of these effects was cytokine-dependent.

Bim mRNA is also known to be regulated in various types of neurons by neurotrophic factors such as NGF [10–12]. Gilley et al. [19] demonstrated that the activity of the promoter of the upstream region of the rat *Bim* gene is 2-fold higher when neuronally differentiated PC12 cells are cultured in the absence of NGF relative to expression detected in the presence of NGF. NGF-dependent promoter activity was disrupted following mutation of a FOXO3a binding site that is conserved in the promoter region between human and rat (Figure 1b, shaded gray). The authors concluded that FOXO3a, a member of the forkhead transcription factor family, plays a key role in downregulation of *Bim* expression by NGF. Therefore, we mutated this binding site (GTAAACA) in the reporter construct (#8) to GTTTTCA. The promoter activity of this mutant (Figure 3b, #22) was even higher than that of the non-mutant construct (#8) in Baf-3 cells, suggesting that FOXO3a is not involved in the transcriptional regulation of *Bim* through this particular site in these cells.

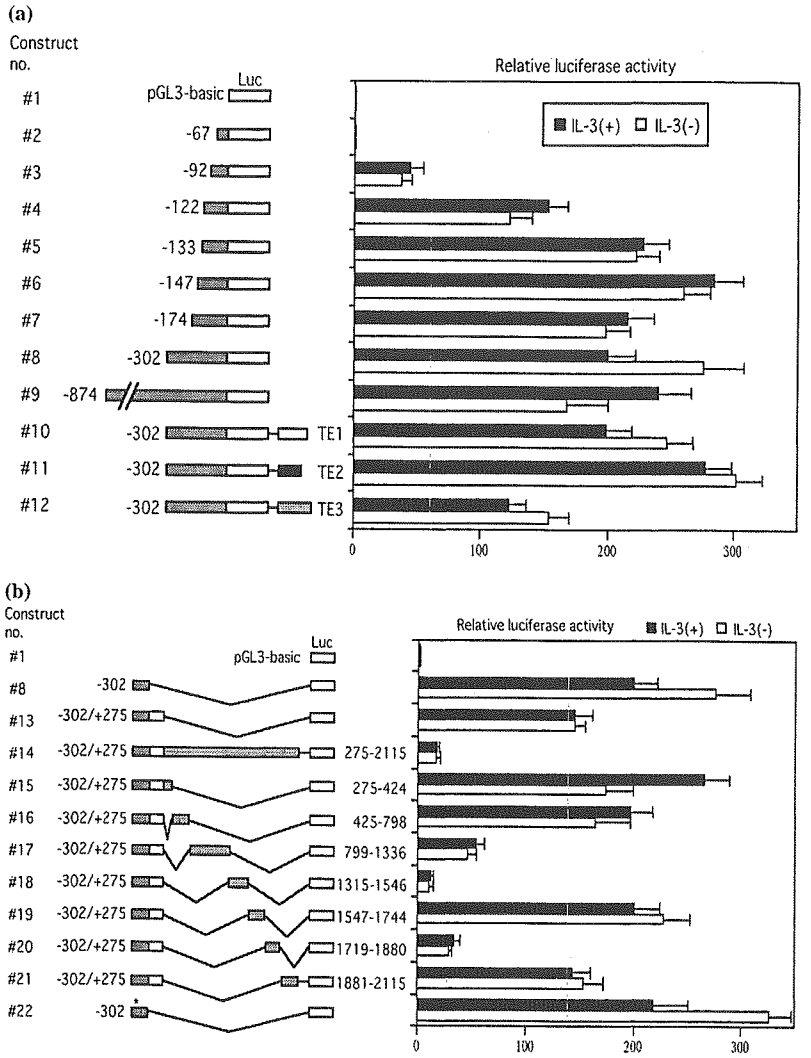

Figure 3. Promoter/enhancer (silencer) activity of candidate *cis*-acting regions of the *Bim* gene. Baf-3 cells were transfected with the indicated reporter plasmid and pRL-tk, as an internal control to normalize luciferase activities for transfection efficiency. Six hours later, cells were divided and were cultured in the presence (black bars) or absence (open bars) of IL-3 for 16 h. The relative luciferase activity was shown. An asterisk (#22) indicates the mutation in the FOXO3a consensus binding site. Each value represents the mean of three independent experiments. The error bars indicate the mean ± the standard deviations.

Equal rate of transcription initiation between IL-3-positive and negative conditions

These data suggested that the induction of *Bim* expression in cytokine-deprived Baf-3 cells is not regulated by a transcriptional mechanism. To confirm this, we performed nuclear run off assays using nuclei isolated from Baf-3 cells cultured in the presence or absence of IL-3. The transcriptional activity of *Bim* was unaffected by IL-3 (Figure 4, lane 2), as was that of the control β-actin gene (lane 4). In contrast, the transcription of

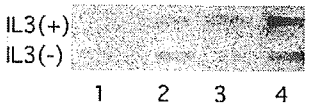

Figure 4. Nuclear run off assay. Nuclei were extracted from Baf-3 cells cultured either in the presence (upper) or absence (lower) of IL-3. mRNA was elongated by incubating nuclei with NTPs and labeling solution for 30 min at 30 °C. RNA was extracted and hybridized to a nylon membrane that contained an empty plasmid vector (lane 1), Bim cDNA (lane 2), Bcl-x_L cDNA (lane 3) and β-actin (lane 4).

Bcl-x_L was increased (lane 3), consistent with previous findings that the transcription of Bcl-x_L is